Cell shape changes during larval body plan development in *Clytia hemisphaerica*

Yulia Kraus[1,2*], Sandra Chevalier[3] and Evelyn Houliston[3*]

1) Department of Evolutionary Biology, Faculty of Biology, Lomonosov Moscow State University, Leninskie Gory 1/12, 119234, Moscow, Russia

2) Koltzov Institute of Developmental Biology of the Russian Academy of Sciences, 26 Vavilov Street, Moscow, 119334, Russia

3) Sorbonne Université, CNRS, Laboratoire de Biologie du Développement de Villefranche-sur-mer (LBDV), 06230 Villefranche-sur-mer, France.

* Corresponding authors: houliston@obs-vlfr.fr , yuliakraus2@gmail.com

Abstract

The cnidarian "planula" larva shows radial symmetry around a polarized, oral-aboral, body axis and comprises two epithelia cell layers, ectodermal and endodermal. This simple body plan is set up during gastrulation, a process which proceeds by a variety of modes amongst the diverse cnidarian species. In the hydrozoan laboratory model *Clytia hemisphaerica,* gastrulation involves a process termed unipolar cell ingression, in which the endoderm derives from mass epithelial-mesenchymal transition (EMT) at the future oral pole of a monoepithelial blastula. This contrasts markedly from the gastrulation mode in the anthozoan cnidarian *Nematostella vectensis*, in which endoderm formation primarily relies on cell sheet invagination. To understand the cellular basis of gastrulation in *Clytia* we have characterized in detail successive cell morphology changes during planula formation by Scanning and Transmission Electron Microscopy combined with confocal imaging. These changes accompany epithialization of the blastoderm, bottle cell formation followed by EMT in the oral domain, cohesive migration and intercalation of ingressed mesenchymal cells, and re-epithelialization of the endoderm. From our data we have reconstructed the cascade of morphogenetic events leading to the formation of planula larva. We also matched the domains of cell morphology changes to the expression of selected regulatory and marker genes expressed during gastrulation. We propose that cell ingression in *Clytia* not only provides the endoderm, but generates internal forces that shape the embryo in the course of gastrulation. These observations help build a more complete understanding of the cellular basis of morphogenesis and of the evolutionary plasticity of cnidarian gastrulation modes.

Key words: gastrulation, hydrozoan, epithelial-mesenchymal transition (EMT), bottle cells, cnidarian, planula

Introduction

Dynamic changes in the shape of individual cells underlie tissue remodeling during many of the morphogenetic events that sculpt the body of metazoan embryos, notably including the key event of gastrulation during which the germ layers and the embryo axes are set up (Solnica-Krezel & Sepich, 2012). Two morphogenetic processes driven by individual cell shape changes are very common during gastrulation: bending of cell sheets (invagination) and cell detachment from epithelia in a process of epithelial-mesenchyme transition (EMT) (Keller & Shook, 2011; Nakaya & Sheng, 2008; Pearl et al., 2017; Shook & Keller, 2003). Both these processes involve transformation of columnar epithelial cells into a wedge shape by constriction of the apical cortex (Hardin & Keller, 1988; Sawyer et al., 2010). At the cellular level such shape changes are driven by regionalized cortical enrichment and activation of myosin (Mason et al., 2013; Sawyer et al., 2010; Sherrard et al., 2010), as well as modulation of cell adhesion molecules and junction proteins to control interactions between neighbors (Buckley et al., 2014; Gutzman et al., 2018; Lecuit & Yap, 2015). Embryonic transcription programs combined with biomechanical feedback mechanisms guide changes in this cellular machinery through embryogenesis, with expression of key transcription factors such as Brachyury, Snail and beta-catenin both directing and responding to these changes (Farge, 2011; Fritzenwanker et al.,2004; Goodwin & Nelson, 2017; Pukhlyakova et al., 2018).

While much attention has focussed on understanding individual morphogenetic processes, much remains to be understood about how these processes coordinate with each other or act 'globally' to shape the embryo (Beloussov, 2015; Heisenberg & Solnica-Krezel, 2008; Leptin & Grunewald, 1990; Miller & Davidson, 2013; Williams & Solnica-Krezel, 2017). This issue of global morphological integration has so far been addressed in relatively few animal models such as nematode (Lee et al., 2006; Marston et al., 2016), *Drosophila* (Holcomb, et al.,2019; Rauzi et al., 2015), amphibians and birds (Firmino et al., 2016; Keller & Winklbauer, 1992; Shook et al., 2018) and ascidians (Sherrard et al., 2010). Much broader phylogenetic sampling will be needed to understand the various mechanisms that integrate morphogenetic movements of embryonic cells, and how this contributes to the evolution of gastrulation modes within the animal kingdom (Stower & Bertocchini, 2017).

Studies in Cnidaria can be very informative for understanding the cellular bases of developmental mechanisms and other morphogenetic processes. They can provide insights not only through comparisons with more traditional experimental model species from Bilateria, but also through

comparisons between cnidarian species, which demonstrate extreme evolutionary and developmental plasticity. This is illustrated nicely by gastrulation, where cnidarians species deploy widely differing modes and cell behaviors to create the cnidarian planula larva (Kraus & Markov, 2017). Cnidaria planulae have a simple diploblastic organization with just two epithelial layers, endoderm and ectoderm organized around a polarised oral-aboral body axis. In some species the inner layer (endoderm) forms principally by cell sheet invagination from a hollow blastula, as described in scyphozoans (Claus, 1890; Berrill, 1949) and anthozoans (sea anemones, some corals: Gemmill & MacBride, 1920; Kraus & Technau, 2006; Magie et al., 2007, Marlow & Martindale 2007). Alternatively, in some hydrozoans and some anthozoans (octocorallians) that develop via a solid morula stage, gastrulation proceeds via germ layer delamination (hydrozoans: Wulfert, 1902; Harm, 1903; Muller-Cale, 1914, Kraus, 2006; Kraus et al., 2014; Burmistrova et al., 2018; anthozoans: Wilson, 1883; Matthews, 1917; Benayahu, 1989; Dahan & Benayahu, 1998). Endoderm can also form exclusively by ingression of individual cells from the future oral pole of the blastoderm, as is the case in *Clytia (=Phialidium)* species (Metchnikoff 1886; Byrum, 2001).

We characterize in detail here cell morphology during embryonic development in *Clytia hemisphaerica. Clytia* exhibits the 'typical' complex life cycle of the class Hydrozoa: The adult stage (medusa) buds asexually from an 'immortal' juvenile stage (polyp colony). The medusa produces gametes daily for external fertilization and the resulting embryo develops into a planula larva. The planula metamorphoses after a few days into a sessile primary polyp, the founder of a new colony (Leclère et al., 2016). *Clytia* is a very useful experimental model for cell and developmental biology as well as evolutionary comparisons, being largely transparent and easy to manipulate in the laboratory. Inbred strains, genomic tools and knockdown techniques are now available (Leclère et al., 2019). The first studies of its embryonic development date back to the nineteenth century, when the mode of gastrulation by ingression of individual presumptive endoderm cells from one pole of the blastula was first described (Metchnikoff, 1886*; C. flavidula* = *C. hemisphaerica*). Using *C. gregarium,* the site of this 'unipolar cell ingression' was later demonstrated experimentally to correspond to the animal pole of the egg (Freeman, 1981), and cell ingression was followed by marking experiments and morphometric analysis (Byrum, 2001). Molecular studies in *C. hemisphaerica* have shown that cell ingression occurs from specialized oral territory established in the blastula by the action of maternally localized mRNAs, which trigger Wnt pathway activation (Momose et al., 2008; Momose & Houliston, 2007). Genes activated downstream of Wnt signaling in this oral domain include orthologs of known gastrulation

regulators, notably two Brachyury orthologues, whose inhibition disrupts gastrulation (Lapébie et al., 2014).

Using *in vivo* imaging, confocal laser scanning microscopy (CLSM), Scanning Electron Microscopy (SEM) and Transmission Electron Microscopy (TEM), we describe here the succession of shape changes for cells of the *Clytia* embryo from cleavage until the planula stage, in relation to their position within the embryo and to the expression domains of selected genes. The characterization of cell shapes in relation to the overall morphology of the embryo during gastrulation allows us to reconstruct the morphogenetic events leading to the formation of planula larva and to predict the forces and tensions generated by the regionalized cell shape changes, ingressions, migrations and intercalations that characterize this particular gastrulation mode.

Materials and Methods

Animals and embryo cultures

Clytia embryos were obtained from laboratory Z strain adults (Leclère et al., 2019). Gametes were collected following light-induced spawning of adult medusae, mixed within one hour to achieve fertilization, and cleaving embryos collected into millipore filtered Red Sea Salt brand artificial sea water (MFSW) for culture. Embryonic development proceeds reliably at temperatures between 17-21°C. Unless otherwise stated we express times of developmental events as hours post fertilization (hpf) at 18°C. Time lapse movies were made using a Zeiss Axiophot-100 or Zeiss AxioObserver inverted microscopes. For early stages embryos were mounted in a small drop of MFSW between two coverslips separated by a moist spacer of filter paper and sealed with silicone grease. At the early gastrula stage the embryos start to swim by beating of ectodermal cilia, so they were embedded in 1.5% low melting point agarose (BioRad) in MFSW in a glass-bottomed petri dish to keep them in the field of view. Note that this does not prevent ciliary beating; the embryos continue to spin with in an agar capsule.

Scanning and transmission electron microscopy (SEM and TEM)

Embryos were fixed overnight at room temperature in the following fixative: one volume of 2.5% glutaraldehyde, four volumes of 0.4 M Na-cacodylate buffer (pH 7,2), and five volumes of microfiltered seawater (1,120 mOsm) (Ereskovsky et al., 2007), and then were transferred into 1.25% glutaraldehyde / 0.2M Na-cacodylate buffer (pH 7.2) and stored at +4°C. Before further processing, samples were post-fixed in 1% OsO4 / 0,2M Na-cacodylate buffer (pH 7,2) for 1 h and washed with the same buffer. Further processing was performed as described in Fritzenwanker et al. (2007). Samples for SEM were examined by the CamScan S-2 and JSM-6380LA scanning electron microscopes. Ultrathin sections were examined by the JEM-1011 transmission electron microscope with a Gatan ES500W Model 782 camera. Electron microscopy was performed at the Electron Microscopy Laboratory of the Biological Faculty (Shared Facilities Centre of M.V. Lomonosov Moscow State University).

Confocal Microscopy

Staining with Hoechst dye and rhodamine-phalloidin of formaldehyde -fixed embryos was performed exactly as described in Momose et al., (2007). Samples were imaged on a Leica SP5 confocal microscope.

In situ hybridization

Single in situ hybridization was performed using DIG labelled antisense probes exactly as described in Lapébie et al (2014). Double in situ hybridization used fluorescein labelled probe for *CheBra1* and a DIG labelled probe for *CheSnail,* detected using Peroxidase and Alkaline phosphatase conjugated antibodies with NBT or Fast red substrates respectively were performed as in (Jager et al., 2011). All genes and probes used here were described in Lapébie et al (2014) except *CheSnail* (accession number MN657238), which we isolated from our EST collection (Chevalier et al., 2006), and *Sox10* (Jager et al., 2011).

Results

Overview of *Clytia* normal development

As outlined in the sister manuscript (van der Sande et al., submitted), the main events of planula morphogenesis are: cleavage, blastocoel formation, blastoderm epithelization, compaction, oral cell ingression, aboralwards endodermal cell migration within the blastocoel, gastrula elongation and re-epithelization of the endoderm. These events are illustrated by light micrographs of the highly transparent embryo in Figs 1 and 2. Cleavage divisions are holoblastic and unipolar, being initiated by nuclei/spindles positioned in the peripheral yolk-poor layer. The first cleavage division occurs about 50 minutes after fertilization and initiates at the animal/oral pole of the zygote, progressing to the aboral pole (Fig. 1A, B). Each subsequent cleavage cycle takes about 30 minutes. Starting from the second cleavage, lamella-like cytoplasmic projections promote close interactions between non-sister blastomeres (Fig. 1C, D). This active "sliding" of blastomeres relative to each other as the cleavage furrows progress promotes packing in configurations which can resemble the spiral cleavage of some bilaterian embryos (Fig. 1E, F). At the 32-cell stage a blastocoel appears (Fig. 1H) defining the blastula stage. The blastocoel expands during the next rounds of synchronous divisions as illustrated at the 128-cell stage in Fig. 1I. The initial shape of a blastula is irregular, but at about 7 hpf as epithelialization commences and individual cells flatten against each other it acquires a more spherical shape.

At the late blastula stage the diameter of the embryo becomes smaller due to a compaction process accompanying epithelialization, and regional differences in the thickness of the blastoderm are first observed (Fig. 2A). At this stage embryos start to swim by beating of cilia on the blastoderm cells, oriented by a conserved planar cell polarity (PCP) mechanism operating along the oral-aboral axis (Momose et al. 2012). The onset of gastrulation is then marked by more pronounced local thickening of the blastoderm, marking the site of cell ingression and future oral pole of the embryo (Fig. 2B, C). As gastrulation progresses, the mass of ingressed cells gradually fills the blastocoel and the front of the mass displaces towards the aboral pole (Fig. 2D - I). This is accompanied by a characteristic change in overall embryo morphology: The oral pole of the gastrula becomes pointed, and the region that contains ingressed cells narrows compared to the more aboral region where the blastocoel is still empty. Around 6 hours after the onset of gastrulation (corresponding to roughly 20 hpf at 18°C), ingression is complete and the blastocoel filled with cells, defining the parenchymula stage (Fig. 2J). Over the next 24 hours gastrulation is completed by reorganization

of the ingressed cells to form an epithelial endodermal layer. A central gastrocoel forms in the central core, and a basal lamina develops separating the germ layers (Fig. 2K - P). Formation of both the gastrocoel and the basal lamina initiate at the aboral pole and progress towards the oral pole (compare images Fig. 2K - O). Differentiation of specific cell types then proceeds and the planula becomes competent to settle and metamorphose at about 72 hpf.

Cellular morphology changes accompanying gastrulation

To understand the changes in cellular cell shape that underlie planula morphogenesis, we examined in detail embryos fixed at successive stages by a combination of Scanning Electron Microscopy (SEM), Transmission Electron Microscopy (TEM), and Confocal Laser Scanning Microscopy (CLSM) following staining of cell boundaries with fluorescent phalloidin and nuclei with Hoechst dye (Figs 3-8).

Blastula stages

The major cellular event during the blastula stage is blastoderm epithelization. Early blastula stages (3 - 6 hpf) have irregular shapes (Fig. 3A, B). At this stage the blastodermal cells are rounded and do not show marked apico-basal polarity, with nuclei positioned in the cell center (Fig. 3B, C). At 6-7 hpf the embryo reaches the mid-blastula stage. Its shape becomes more regular, and cells show the first sign of apico-basal polarity as their nuclei displace towards the embryo surface (Fig. 3D). At this stage cell divisions become asynchronous. Cells flatten with respect to each other and start to adopt a columnar shape, but do not yet show pronounced elongation along the apico-basal axis (Fig. 3D, E). At about 7 hpf, the shape of an embryo is almost spherical (Fig. 3F, H). Cilia appear on the cell apical surfaces (Fig. 3G). All blastodermal cells are now clearly columnar (Fig. 3H, I, J, K), but the shape of individual cells is not uniform. In some cells the lateral surfaces are roughly parallel while in others the basal surfaces are either expanded or reduced relative to the apical surfaces (Fig. 3I, J, K). At the late blastula stage (8–10 hpf), blastodermal cells become more markedly columnar, with the apicobasal-axis:apical-width ratio reaching about 3:1 (Fig. 3L).

The cell shapes characterized in the blastula and in different regions of the embryos during successive stages of planula development, as described in the following sections, are summarized schematically in Figure 4.

Early gastrula stages - bottle cell formation

Starting around 9 hpf, the blastoderm becomes thicker on one side of the late blastula, marking the future position of the oral pole. This thickened oral area is variable in size, and can contain either one or two main patches of ingressing cells. The thickening of the oral pole blastoderm becomes pronounced at the onset of gastrulation (10 - 11 hpf; compare oral (top) and aboral (bottom) regions in Figs. 5A, B, C). Examination of cellular morphology within the thickened oral pole (Figs. 5B, E and 6A', B) reveals a mixture of cell shapes, classifiable into two types of morphology. Cells of the first type (colored in yellow in Fig. 6) have short apico-basal axes and are columnar or wedge shaped. These are ordinary epithelial cells. Cells of the second type (colored in violet in Figs. 4, 5 and 6) have elongated apico-basal axes, expanded basal domains and frequently a reduced apical width. These features classically characterize 'bottle cells'. We found that bottle cells in *Clytia* form in an oral territory covering up to one third of the early gastrula. Within this territory ordinary epithelial cells alternate with forming bottle cells (Figs. 5b, e and 6a', b).

Across the rest of the embryo, corresponding to future aboral and lateral regions of the early gastrula, wedge-shaped or columnar cells (Fig. 5G) also alternate with cells with expanded basal domains (Fig. 5A, C, F). As in the oral domain, the apical cell surface areas are variable (Fig. 5D), and many cells have expanded basal domains and reduced apical widths. The “basally expanded” cells in aboral/lateral regions did not show increased elongation along the apicobasal axis, distinguishing them from the true bottle cells observed in the oral domain. The nuclei of most aboral/lateral cells at this stage were located within the apical half of the cell, occupying surface or medial positions. TEM revealed that storage vesicles enriched in yolk are concentrated basal to the nucleus in all cells (Fig.5G). These comparisons of cell morphology across the embryo indicate that local thickening of the oral blastoderm prior to gastrulation is caused by apico-basal elongation of a sub-population of cells undergoing bottle cell formation.

Within the oral domain, the widely variable morphologies of bottle cells (eg cells marked in turquoise in Fig. 5A,B,H, Fig. 6A, see also cartoon in Fig. 4B) correspond to stages of a typical process of EMT (Shook & Keller, 2003). Since EMT of these cells is not synchronized within the blastoderm, nearby cells are observed at different stages of the process, finally detaching individually from the epithelial layer to become mesenchymal (Fig. 5E). Close examination of the apical surface revealed that as ingressing bottle cells sink into the blastocoel, (Fig. 6C - F), protrusions from epithelial cells surrounding the sinking bottle cells and cover their apical surfaces. In this way new junctional complexes between the neighboring cells ensure that the epithelial sheet remains sealed as the ingressing cells detach into the blastocoel (Fig. 6E, F, J). It is notable that in

Clytia embryos bottle cells retain their epithelial characters, including cilia and apical junctions, during almost the entire process of ingression. This likely reflects the importance for survival of maintaining a strong apical seal between all cells during gastrulation, separating the external seawater from the blastocoelar space.

From electron microscope data we can detail successive stages of bottle cell formation (Fig. 6; schematized in Fig. 4B). First, the apical surface contracts slightly and the apico-basal starts to elongate. Concurrently, the basal part expands and a narrow neck forms, connecting distinct apical and the basal domains (Fig. 6B, K, L). At this stage the nucleus is located in the cell neck (Fig. 6B). At the next step, the apical surface of the bottle cell progressively reduces, and the neck becomes narrower (Fig. 6J, M). Constriction of the cell apical domain appears to force the cytoplasm and nucleus towards the basal domain. Cytoplasmic components become deformed along the apico-basal axis (such as the vacuoles in Fig. 6H) or align along the neck (such as the storage vesicles in Fig. 6G). The nucleus then displaces from the neck to the expanded basal part of the cell (Fig. 6G). Interestingly, ingressing cells retain their sub-apical junctions and cilia during most of the ingression process, even when the apical surface is reduced to a very small area (Fig. 6F, H, I, N). At the next step, the apex of bottle cell contracts further, while the neck region becomes narrower and slightly shorter (Fig. 6N, J). Due to extreme contraction of the cell apex, cytoplasmic components located near the apical surface, such as the cortical granules in the Fig. 5I, move deeper, while sub-apical junctions are still retained in the bottle cells (Fig. 6I). Finally, the neck of the bottle cell contracts (Fig. 6O), intercellular junctions are lost and the cell leaves the epithelium (Figs. 5B ; 6P, J). In the course of EMT, the leading and trailing edges of each bottle cell adopts morphological features typical of migrating cells (Fig. 6B, G, M, P). However, only few filopodial or lamellipodial protrusions are detected at the leading edge (former basal surface) (Fig. 6M-O). These morphological observations suggest that bottle cells drop out of the oral blastoderm principally as a result of cell shape changes, and only start to migrate once in the blastocoel.

Ingressed cells have a typical mesenchymal phenotype indicating that they move actively by crawling on the blastocoel wall and neighboring cells (Fig. 5H -J). Cells migrating over the blastocoel wall develop very pronounced leading edges with wide lamella adorned with multiple filopodiae (Fig. 5I). These cells crawl towards the aboral pole of an embryo. Cells located further from the blastocoel wall use other ingressed cells as a substrate for crawling. They form small lamella and multiple filopodiae (Fig. 6J).

Mid-gastrula stage

During mid-gastrula stages, embryos adopt a characteristic pear shape as the part of the embryo in which the ingressed cells have entered the blastocoel becomes thinner. The embryo can thus be divided into two distinct parts, a rounded aboral part and a thinner, more pointed, oral part (Fig. 7A-D). The behavior of the ingressed cells during mid-gastrula stages appears highly coordinated. Flattened mesenchymal cells displace as streams or cohesive blocks in which cells are oriented end-to-end and side-to-side, aligning as layers perpendicular to the oral-aboral axis (Fig. 6C-E). The morphology and arrangement of these cells inside the blastocoel indicates that central cells migrate relative to each other and intercalate along the elongating oral-aboral axis (Fig. 6E, F, G), while those close to the blastocoel wall migrate along it towards the aboral pole (Fig. 6I, J, L). Migrating cells form multiple spot-like sites of adhesion resembling the cell-substrate focal contacts characteristic for mesenchymal cells migrating in culture (Fig. 6H). This coordinated behavior of the ingressed cells likely accounts for the global pear-shaped morphology mid-gastrula stage embryos, with their intercalation reducing the diameter of the oral region. Consistently, disruption of cell intercalation orthogonal to the oral-aboral axis by morpholino-knockdown of PCP proteins (Momose et al., 2012) or as modelled in silico (van der Sande et al, submitted), prevents the narrowing of the embryo during gastrulation.

The non-ingressing cells of the blastoderm also show distinct morphologies during mid-gastrula stages. In lateral regions, forming a belt at the level of the underlying front of cell ingression, they become slanted or skewed, with their apicobasal axes bent towards the embryo oral pole (Fig. 7I-L). We hypothesize that this results from the pulling forces exerted by prospective endoderm cells migrating along the underlying blastocoel roof (see Discussion). Another distinct behavior of blastoderm cells, observed across all of the rounded oral part of the gastrula, results in its stratification during mid and late gastrula stages. The nuclei of a scattered cell sub-population displace basally as gastrulation proceeds, such that a layer of nuclei forms progressively on the basal side of the blastoderm (Fig. 7L, 8E). It appears that these nuclei belong to a distinct layer of flattened cells lining the blastocoel, but we cannot rule out that thin apical projections connect these cells to the embryo surface. Finally, some mitotic blastoderm cells are observed throughout gastrulation, typically rounding up and adopting apical positions during division (Fig. 8E).

Late gastrula stage

At the late gastrula stage (Fig. 8) gross morphological differences between the oral and aboral parts of the embryo progressively diminish. During this period the embryo surface becomes very uneven

and covered with wrinkles (Fig. 8A, B, D, F, G, H, I). At the oral pole the ratio of bottle cells to epithelial cells gradually decreases as gastrulation progresses. However, we found bottle cells even at the late gastrula stage (Fig. 8B, C), indicating that they continue to be generated over an extended time period in *Clytia*. Mesenchymal cells aligned perpendicular to the oral-aboral axis could still be detected in the central core of ingressing cells throughout gastrulation, but become progressively fewer as the embryo narrows and are mainly confined to the front of the advancing cell mass (Fig. 8D, E). Conversely, flattened cells aligning with and migrating upon the blastoderm wall remain a major feature until gastrulation is complete. In the blastoderm, the abundant wrinkles overly regions or migrating cells (Fig. 8F, G) and the some blastoderm cells slant into the wrinkles from both sides (Fig. 8I, J, K, N). The end of cell ingression, at about 24hpf, marks the parenchymula stage, from which point the embryonic surface morphology becomes smooth again (Fig. 8L, Fig 9B).

Planula development from the parenchymula; endodermal cell epithelialization.

During the 24 hours following the completion of cell ingression (Fig. 9A-G), the main event of planula morphogenesis is the reorganization of ingressed cells to form an endodermal epithelial layer. This is accompanied by two major cellular processes, both of which start from the aboral pole and proceed orally. One is the formation of a gastrocoel. This cavity is created by massive death of cells in the central core of the planula, detectable as nuclear fragmentation and loss of cell integrity (Fig. 9A,C,E,G,H). The second is structuring of those ingressed cells close to the blastocoel wall into an epithelium of columnar cells, a process accompanied by the appearance of a distinct basal lamina separating the ectodermal and endodermal epithelia (Fig. 9E,G.,H). This lamina stains strongly with phalloidin because of actin-rich contractile projections that develop on the basal surface of the differentiating epitheliomuscular that predominate in both layers. Cilia on each ectodermal epithelial cell are positioned towards the oral side (Fig. 9K) as described previously (Momose et al., 2012).

In parallel to endoderm epithelialization, cell type diversification is observed in the outer layer of the planula as the blastoderm transforms into a more complex ectodermal epithelium, this process becoming complete between two and three days after fertilization. The richer variety of cell types, including nematocytes, neural cells and secretory gland cells (Bodo and Bouillon, 1968) is reflected by greater heterogeneity of cell morphology and nuclear position (Fig. 9G,H,J,L).

Gene expression changes accompanying gastrulation

To help understand how the cell morphological changes observed during gastrulation relate to regionalized expression of regulatory genes we performed in situ hybridization on embryos fixed at successive stages (Fig. 10A). Two *Clytia* brachyury genes, *CheBra1* and *CheBra2,* are expressed downstream of the oral Wnt3 signaling that defines the oral /endodermal domain at the early gastrula stage (Momose & Houliston, 2007; Momose et al., 2008; Lapébie et al., 2014). We detected *CheBra1* and *CheBra2* expression in overlapping cell populations within the oral domain of the blastoderm before and during gastrulation, and finally of the planula ectoderm, but not in ingressed cells (Fig. 10A, B). These two *Clytia* brachyury paralogues appear to have partly redundant functions in gastrulation (Lapébie et al., 2014), but may have more distinct roles in adult stages as shown for their orthologues HyBra1(endodermal) and HyBra2 (ectodermal) in the *Hydra* polyp oral pole region (Bielen et al., 2007). The *Clytia* orthologue of Snail, a transcriptional repressor implicated in EMT as well as cohesive cell migration across many species and developmental contexts (Barrallo-Gimeno & Nieto, 2005), showed a dynamic expression pattern. It was detectable in cells across the entire blastoderm in late blastula stages, before becoming concentrated more orally at the onset of gastrulation. During these stages, expression of *CheSnail, CheBra1* and *CheBra2* all showed a small local reduction at the oral pole (Fig. 10A, B). In mid-gastrula stage embryos, detectable *Snail* expression became confined to ingressing and internalised cells, notably ones at the front of the migrating cell mass, and by planula stages *CheSnail* expression was only weakly detectable (Fig. 10A).

Expression of the *Clytia FoxA* transcription factor (Lapébie et al., 2014), whose orthologues are associated with the development of digestive territories in many animal species (Steinmetz et al, 2017), was detected in oral domain cells from the early gastrula stage. The number of *CheFoxA* expressing cells diminished progressively as gastrulation proceeded. They were initially concentrated in the blastoderm and showed bottle-cell like morphology with constricted apical domains. FoxA positive cells were later also detected in oral region of the developing endodermal mass, this distribution presumably corresponding to early-internalised cells (Fig. 10A, C). By the planula stage *FoxA* expression was no longer detectable. Conversely the *Clytia*-specific endoderm marker gene *WegIE2* (Lapébie et al., 2014) became detectable in more aboral regions of the internalized cell mass, consistent with a switch in expression between these two genes in the course of endoderm cells differentiation.

Finally, expression of the Sox10, a B type Sox transcription factor expressed in neural cells of the adult *Clytia* medusa (Jager et al., 2011), was detected throughout the blastoderm except in the oral

pole ingressing cells (Fig. 10A,C). Expression persisted in the basal region of lateral and aboral ectoderm cells until the end of gastrulation. Residual expression could be detected in a basal domain of the aboral pole ectoderm at the parenchymula stage. This Sox10 expression pattern coincides with the accumulation of basal nuclei the lateral blastoderm during nuclear stratification described in Fig. 7M, 8E., suggesting that cells with a neural fate are generated in this position.

Discussion

We have reconstructed the changes in cell shape, cellular behavior and underlying ultrastructure associated with successive stages of gastrulation in *Clytia hemisphaerica,* as summarized in Figure 4. These transform a simple blastula comprising an irregular mono-epithelial ball into an elongated, polarized, planula larvae with two structured epithelia, endodermal and ectodermal. Cell heterogeneity first arises across the whole embryo at the blastula stage, accompanying epithelialization and "compaction" of the blastoderm layer (Fig. 4A,Ba). Elongated cells with a bulbous basal region arise, interspersed with shorter cells tapered to a basal point ("squat cells"). Bottle cell formation, culminating in individual cell ingression via EMT, then occurs asynchronously within an oral domain throughout the gastrulation period (Fig. 4B,C). As the blastocoel fills, the whole embryo elongates and adopts pear shaped morphology, with characteristic constriction of the developing ectodermal layer in a belt region overlying the migration and wrinkling in lateral regions associated with concerted bending of the basal domains of the epithelized cells (Fig. 4D, E). Finally, as the parenchymula adopts its smother, pointed torpedo shape, the inner mass of cells reorganize into epithelial layer in an aboral-oral progression, and an extracellular mesoglea is elaborated to separate the basal surfaces of the two epithelia (Bodo and Bouillon, 1968; Fig. 4G, H). The elaboration in this layer of myofibrillar foot processes that extend from differentiating epithelial cells, intermixed with neurites projecting from neurosensory and ganglionic cells (Lapébie et al., 2014; Thomas et al., 1987), also progresses from aboral to oral (Gröger & Schmid, 2001).

The morphology of a developing embryo and of the cells within it are intimately linked. The particular mechanical environment of the embryo influences how individual cells behave, while conversely cell behavior influences the mechanics of tissues and of the whole embryo (LeGoff & Lecuit, 2015). Indeed, mechanical forces can be considered among the primary coordinators of morphogenetic process, with cell behavior being guided by forces transmitted over long range (Heisenberg & Bellaïche, 2013). Below we attempt to interpret embryo morphology during *Clytia* planula formation in terms of forces and tensions generated by collective cellular movements and shape changes of distinct cell sub-populations

Setting up cell morphology differences ahead of gastrulation

As discussed in detail in the accompanying manuscript (van der Sande et al., submitted), the generation of two equivalent cell forms from an initially uniform epithelial population during

compaction of the *Clytia* blastula is likely a consequence of apical constriction in all cells, as predicted using a 2D model based on cell boundary forces. An equivalent segregation of cell morphologies was reported for cells at the onset of gastrulation in *Nematostella* (Tamulonis et al., 2011), although in this species it is restricted to the oral domain of presumptive endoderm cells. "Basally expanded" cells located in the oral domain (presumptive endoderm) likely provide the basis for bottle cell formation in both species. Those in lateral/aboral regions (presumptive ectoderm) in *Clytia* may rather contribute to generating a distinct basal layer of the blastoderm via a process of stratification /pseudostratification. This idea remains to be demonstrated experimentally, but is supported by the transient expression in basal regions of the blastoderm of the transcription factor Snail, and subsequent expression of the neurogenesis-related transcription factor Sox10 (Fig. 9; Jager et al., 2011). Generation of a basal blastoderm layer has also been observed in the hydrozoan *Gonothyraea loveni,* in this case via oriented cell divisions (Burmistrova et al., 2018).

Snail, Bracyhury and FoxA/Forkhead transcription factors are associated with gastrulation in many animal species and contribute to regulating cell morphology changes. Clade-specific roles in developmental fate determination may have been acquired secondarily. In this context it can be informative to compare their expression patterns in *Clytia* and in the anthozoan cnidarians *Nematostella* and *Acropora*, which gastrulate principally by cell sheet invagination and involution rather than ingression. In both cases Wnt/ß catenin signaling in the blastula defines an oral domain of gene activation to initiate these events (Lapébie et al., 2014; Röttinger et al., 2012). Brachyury gene expression patterns within these domains show similar features, either condensing as a ring ahead of blastopore lip formation in N*ematostella* and *Acropora* (Scholz & Technau, 2003; Fritzenwanker et al., 2004; Hayward, et al., 2015; Magie et al., 2007) or in a more salt-and-pepper distribution anticipating cell ingression in *Clytia*. Interestingly these patterns match the observed distribution of bottle cells, as well as that predicted by 2D cell-boundary-based models of gastrulation (Tamulonis et al., 2011). We can speculate that Brachyury transcription factors participate in maintaining cortical constriction in both models, contributing to the initial stages of bottle cell formation via apical constriction in *Clytia,* and inward rolling of the blastopore lip in *Nematostella*. The resultant stress in these cells may contribute to maintenance of Brachyury expression until they ingress (in *Clytia*) or stop involuting movement (in *Nematostella*) via biomechanical feedback mechanisms, as suggested by experiments in *Nematostella* (Pukhlyakova et al., 2018), This is consistent with the idea of an ancestral role for Brachyury in blastopore formation -or its equivalent as the site of cell ingression in *Clytia* embryos (Gross & McClay, 2001; Hayward et al., 2015; Marcellini et al., 2003; Scholz & Technau, 2003; Technau, 2001). The 2D

models for *Nematostella* and *Clytia* gastrulation predict that a second key feature to drive endoderm formation in both cases is modulation of the strength of cell adhesion (Tamulonis et al., 2011). Adhesion between oral-domain blastoderm cells is downregulated at the onset of gastrulation and then weakly promoted between the internalised presumptive endoderm cells. Snail transcriptional regulators are strong candidates to mediate these adhesion changes. In *Nematostella* and *Acropora* Snail-expressing cells form the blastopore 'floor' which undergo a 'partial' EMT, and then following invagination they transform progressively into endoderm (Fritzenwanker et al., 2004; Hayward et al., 2015; Magie et al., 2007). These successive morphogenetic changes have been shown to be tightly linked to modulation of the expression of two cadherin genes in *Nematostella* (Pukhlyakova et al., 2019). In *Clytia*, Snail expressing cells are scattered through the oral domain at the onset of gastrulation and undergo complete EMT, before migrating together aborally as a cohesive unit. Many equivalent cell behaviors during gastrulation in other species, including the cohesive cell migration of fish involuting mesendoderm cells and EMT of presumptive mesoderm cells from the chick epiblast, involve Snail-dependent regulation of cell adhesion and migration (Barrallo-Gimeno & Nieto, 2005; Savagner, 2001).

FoxA(=Forkhead) expression profile comparisons between species are suggestive of involvement in fate determination rather than mainly in morphogenetic movements. *NvFoxA* is expressed early during blastopore formation in the same domain as *NvBra* (Fritzenwanker et al., 2004; Magie et al., 2007), later giving rise to the pharyngeal ectoderm. Cells of his domain will develop exocrine digestive functions, linking it evolutionarily to endoderm domains in bilaterian species (Steinmetz, 2019; Steinmetz et al., 2017). In contrast *Amfkh* is only transiently expressed in the developing blastopore, and this pattern is spatially and temporally separated from its later expression in the pharynx (Hayward et al., 2015). In *Clytia*, FoxA is transiently expressed in bottle cells, but the fate of these cells is not yet known. It will be interesting to determine whether these FoxA expressing cells give rise to any particular endodermal cell type.

Forces and tensions sculpting embryo morphology during gastrulation

Mid and late stage gastrula embryo provide a complex landscape for inferring tissue forces and tensions from embryo and cell morphologies, as schematized in Fig. 11. As the ingressed cells fill the blastocoel, they form three populations: a "shell" of tightly-associated flattened cells crawling along the blastocoel wall, flattened intercalating cells in the "core" oriented perpendicular to the oral-aboral axis, and a less ordered core population closer to the oral pole (Fig 11B, C). In concert

the embryo shape changes markedly - the oral area progressively narrows and becomes pointed (Fig. 7A; Fig. 11 Ba, Ca), while the locally constricted “belt” zone of the blastoderm accompanies the front of underlying cells migrating towards the aboral pole (Fig. 7B; Fig. 11Ba, Bb). We propose that embryo morphology is dictated primarily by the shell cells and the intercalating core cells. The migrating shell cells are predicted to generate the blastodermal folds beneath and behind them, as well as tension lines in front of them that in turn guide migration. These cells associate closely with each other (see spots of adhesion in Fig. 7H) and appear to migrate aboralwards as a cohesive structure (dark blue arrows in Fig. 11Bd, Ce). The coherent movement of the cells at the aboral front of migration resembles that of 'leader' cells during wound healing (du Roure et al., 2005; Poujade et al., 2007). Forces generated by the actin cytoskeleton of migrating cells generate wrinkles in the substrate (Fournier et al., 2010), in this case on the blastocoel wall (Fig.11 Bd, D, E). Compression of the *Clytia* blastocoel wall beneath and behind the migrating cells into a mass of microscopic folds, oriented perpendicular to the direction of cell migration (Fig. 11 C, F), could result from amplification of wrinkles as accumulating deformations create additional mechanical stresses (Lange & Fabry, 2013; Moeendarbary & Harris, 2014). In contrast, the blastocoel wall ahead of the collectively migrating cells becomes stretched into radiating folds oriented along the lines of tension (Fig.11 D, E, Cb, e), as has been demonstrated using artificial deformable substrates (Harris et al., 1980; Pelham & Wang, 1999). These lines of tension are good candidates to orient the migration of the shell cells along the oral-aboral axis (Lange & Fabry, 2013; Tambe et al., 2011).

The second cell population of key importance to gastrula morphogenesis comprises flattened mesenchymal cells stacked along the oral-aboral axis towards the front of the advancing core (dark violet cells in Fig.11 B, C), (Fig. 4D, E). Their organization and morphology is highly reminiscent of involuting mesoderm cells that intercalate towards the midline during chordate gastrulation (Wallingford et al. 2002). In both cases, narrowing of the internal internalizing cell mass and the associated embryo elongation, is disrupted by knockdown of the PCP proteins (Momose et al., 2012). The 2D model of *Clytia* gastrulation (van der Sande et al, submitted). indicates that lateral crawling interactions between the ingressed cells make an important contribution to embryo elongation. PCP-depended lateral intercalation between cells of the blastoderm also likely contributes (Byrum, 2001; Momose et al., 2012). Another consequence of intercalation between ingressing endoderm cells, also suggested by Byrum (2001), is the narrowing of the oral region during gastrulation. Forces generated in the front portion of the ingressing mass pull the blastocoel wall towards the center leading to formation of the constricted “belt”(Fig.11 B).

A third, more disordered, cell population arises in oral regions of the core during gastrulation as further cells ingress (Fig. 11 Cb). We propose that most of these cells initially join the core rather than the shell because the layers of aligned core cells are under tension and thus attract newly ingressed migrating cells (Lo et al., 2000). In contrast, by the end of gastrulation, ingressing cells will rather join the stiffened shell that is under the strong tension at this stage. The much reduced diameter of the parenchymula reflects both loss of cells from the blastoderm and lateral intercalation of the core cells. Diameter reduction in turn leads to reduction of tension inside the core (Fig.11 Cd). At the same time, diameter reduction generates squeezing forces perpendicular to the OA axis and contributes to the aboralward displacement of ingressed cells (Fig.11 Cd). The polarized morphology of the canonical hydrozoan larva, including its pronounced elongation and tapered posterior end emerges towards the end of gastrulation (Fig.11 C).

Future studies will be required to test these predictions about forces tensions and cell behavior. One approach would be to target the molecular and cellular mechanisms of both individual cell shape changes and overall physical properties. For instance, adhesion molecules and ECM components contributing to the cohesive migratory behaviors of the cells could be tested by downregulation of candidate cell surface molecules expressed in these cells, or signaling molecules expressed in the oral and aboral ectoderm (Lapébie et al., 2014). It would also be interesting to test the importance of localized relaxation and contraction of the actomyosin cortex of different cell populations using optogenetics approaches (Krueger et al., 2018).

Conclusions

Overall our study highlights how cell ingression and in particular the migration of ingressing cells relative to each other and to the blastocoel wall in *Clytia* not only provides the material to form the endodermal germ layer, but also generates forces that shape the embryo in the course of gastrulation. The polarized morphology of the canonical hydrozoan larva, including elongated shape and tapered posterior end, is thus tightly linked to the cell morphological processes accompanying unipolar ingression, followed by migration and PCP-mediated interactions of the internalized cells.

Acknowledgements

We thank all our research colleagues for their useful comments. We also thank Alexandre Jan and Laurent Gilletta for animal maintenance. Experimental work was supported by core CNRS and Sorbonne University funding to the LBDV. The Marine Resources Centre (CRBM) and PIV imaging platform of Institut de la Mer de Villefranche (IMEV) used in this study are supported by EMBRC- France (#ANR-10-INBS-02). We are very grateful to the Electron Microscopy Laboratory of the Shared Facilities Center of the Moscow State University for great help and support. Y.K. research work was supported by federal project 0108-2019-0003 of the Koltzov Institute of Developmental Biology of the Russian Academy of Sciences

References

Barrallo-Gimeno, A., & Nieto, M. A. (2005). The Snail genes as inducers of cell movement and survival: implications in development and cancer. *Development* , *132*(14), 3151–3161.

Beloussov, L. V. (2015). Morphogenesis on the Multicellular Level: Patterns of Mechanical Stresses and Main Modes of Collective Cell Behavior. In L. V. Beloussov (Ed.), *Morphomechanics of Development* (pp. 75–111). Cham: Springer International Publishing.

Benayahu, Y. (1989). Reproductive Cycle and Developmental Processes During Embryogenesis of *Clavularia hamra* (Cnidaria, Octocorallia). *Acta Zoologica* , *70*(1), 29–36.

Berrill, N. J. (1949). Developmental analysis of scyphomedusae. *Biological Reviews of the Cambridge Philosophical Society*, *24*(4), 393–410.

Bielen, H., Oberleitner, S., Marcellini, S., Gee, L., Lemaire, P., Bode, H. R., … Technau, U. (2007). Divergent functions of two ancient Hydra Brachyury paralogues suggest specific roles for their C-terminal domains in tissue fate induction. *Development* , *134*(23), 4187–4197.

Bodo, F and Bouillon, J. 1968. Etude histologique du développement embryonnaire de quelques Hydroméduses de Roscoff. Cahiers de Biologie Marine IX: 69–79.

Buckley, C. D., Tan, J., Anderson, K. L., Hanein, D., Volkmann, N., Weis, W. I., … Dunn, A. R. (2014). Cell adhesion. The minimal cadherin-catenin complex binds to actin filaments under force. *Science*, *346*(6209), 1254211.

Burmistrova, Y. A., Osadchenko, B. V., Bolshakov, F. V., Kraus, Y. A., & Kosevich, I. A. (2018). Embryonic development of thecate hydrozoan Gonothyraea loveni (Allman, 1859). *Development, Growth & Differentiation*, *60*(8), 483–501.

Byrum, C. A. (2001). An Analysis of Hydrozoan Gastrulation by Unipolar Ingression. *Developmental Biology*, Vol. 240, pp. 627–640. https://doi.org/10.1006/dbio.2001.0484

Chevalier, S., Martin, A., Leclère, L., Amiel, A., & Houliston, E. (2006). Polarised expression of FoxB and FoxQ2 genes during development of the hydrozoan *Clytia hemisphaerica. Development Genes and Evolution*, *216*(11), 709–720.

Claus, C., 1890. Ueber die Entwicklung des Scyphostoma von *Cotylorhiza, Aurelia,* und *Chrysaora,* sowie ueber die systematische Stellung der Scyphomedusen. Arb. Zool. Inst. Univ. Wien 9, 85–128.

Dahan, M., & Benayahu, Y. (1998). Embryogenesis, Planulae Longevity, and Competence in the Octocoral Dendronephthya hemprichi. *Invertebrate Biology: A Quarterly Journal of the American Microscopical Society and the Division of Invertebrate Zoology/ASZ*, *117*(4), 271–280.

du Roure, O., Saez, A., Buguin, A., Austin, R. H., Chavrier, P., Silberzan, P., & Ladoux, B. (2005). Force mapping in epithelial cell migration. *Proceedings of the National Academy of Sciences of the United States of America*, *102*(7), 2390–2395.

Farge, E. (2011). Mechanotransduction in development. *Current Topics in Developmental Biology*, *95*, 243–265.

Firmino, J., Rocancourt, D., Saadaoui, M., Moreau, C., & Gros, J. (2016). Cell Division Drives Epithelial Cell Rearrangements during Gastrulation in Chick. *Developmental Cell*, *36*(3), 249–261.

Fournier, M. F., Sauser, R., Ambrosi, D., Meister, J.-J., & Verkhovsky, A. B. (2010). Force transmission in migrating cells. *The Journal of Cell Biology*, *188*(2), 287–297.

Freeman, G. (1981). The cleavage initiation site establishes the posterior pole of the hydrozoan embryo. *Wilhelm Roux's Archives of Developmental Biology*, *190*(2), 123–125.

Fritzenwanker, J. H., Saina, M., & Technau, U. (2004). Analysis of forkhead and snail expression reveals epithelial–mesenchymal transitions during embryonic and larval development of Nematostella vectensis. *Developmental Biology*, *275*(2), 389–402.

Gemmill, J. F., & MacBride, E. W. (1920). IX.—The development of the sea-anemones Metridium dianthus (Ellis) and Adamsia palliata (Bohad). *Philosophical Transactions of the Royal Society of London. Series B, Containing Papers of a Biological Character*, *209*(360-371), 351–375.

Goodwin, K., & Nelson, C. M. (2017). Generating tissue topology through remodeling of cell-cell adhesions. *Experimental Cell Research*, *358*(1), 45–51.

Gröger, H., & Schmid, V. (2001). Larval development in Cnidaria: a connection to Bilateria? *Genesis* , *29*(3), 110–114.

Gross, J. M., & McClay, D. R. (2001). The role of Brachyury (T) during gastrulation movements in the sea urchin *Lytechinus variegatus*. *Developmental Biology*, *239*(1), 132–147.

Gutzman, J. H., Graeden, E., Brachmann, I., Yamazoe, S., Chen, J. K., & Sive, H. (2018). Basal constriction during midbrain-hindbrain boundary morphogenesis is mediated by Wnt5b and focal adhesion kinase. *Biology Open*, *7*(11). https://doi.org/10.1242/bio.034520

Hardin, J., & Keller, R. (1988). The behaviour and function of bottle cells during gastrulation of *Xenopus laevis*. *Development* , *103*(1), 211–230.

Harris, A., Wild, P., & Stopak, D. (1980). Silicone rubber substrata: a new wrinkle in the study of cell locomotion. *Science*, Vol. 208, pp. 177–179. https://doi.org/10.1126/science.6987736

Harm, K., 1903. Die Entwicklung von *Clava squamata.* Z. Wiss. Zool. 73, 115–165.

Hayward, D. C., Grasso, L. C., Saint, R., Miller, D. J., & Ball, E. E. (2015). The organizer in evolution–gastrulation and organizer gene expression highlight the importance of Brachyury

during development of the coral, Acropora millepora. *Developmental Biology*, *399*(2), 337–347.

Heisenberg, C.-P., & Bellaïche, Y. (2013). Forces in tissue morphogenesis and patterning. *Cell*, *153*(5), 948–962.

Heisenberg, C.-P., & Solnica-Krezel, L. (2008). Back and forth between cell fate specification and movement during vertebrate gastrulation. *Current Opinion in Genetics & Development*, *18*(4), 311–316.

Holcomb, M. C., Gao, G. J. J., Servati, M., & Schneider, D. (2019). Mechanical Feedback and Robustness of Apical Constrictions in Drosophila Embryo Ventral Furrow Formation. *bioRxiv*. https://www.biorxiv.org/content/10.1101/743609v1.

Jager, M., Quéinnec, E., Le Guyader, H., & Manuel, M. (2011). Multiple Sox genes are expressed in stem cells or in differentiating neuro-sensory cells in the hydrozoan Clytia hemisphaerica. *EvoDevo*, *2*, 12.

Keller, R., & Shook, D. (2011). The bending of cell sheets-from folding to rolling. *BMC Biology*, *9*, 90.

Keller, R., & Winklbauer, R. (1992). Cellular basis of amphibian gastrulation. *Current Topics in Developmental Biology*, *27*, 39–89.

Kraus, Y. A., & Markov, A. V. (2017). The gastrulation in Cnidaria: A key to understanding phylogeny or the chaos of secondary modifications? *Biology Bulletin Reviews*, 7(1), 7–25. https://doi.org/10.1134/S2079086417010029

Kraus, Y., Flici, H., Hensel, K., Plickert, G., Leitz, T., & Frank, U. (2014). The embryonic development of the cnidarianHydractinia echinata. *Evolution & Development*, Vol. 16, pp. 323–338. https://doi.org/10.1111/ede.12100

Kraus, Y., & Technau, U. (2006). Gastrulation in the sea anemone Nematostella vectensis occurs by invagination and immigration: an ultrastructural study. *Development Genes and Evolution*, *216*(3), 119–132.

Krueger, D., Tardivo, P., Nguyen, C., & De Renzis, S. (2018). Downregulation of basal myosin□II is required for cell shape changes and tissue invagination. *The EMBO Journal*. Retrieved from https://www.embopress.org/doi/abs/10.15252/embj.2018100170

Lange, J. R., & Fabry, B. (2013). Cell and tissue mechanics in cell migration. *Experimental Cell Research*, Vol. 319, pp. 2418–2423. https://doi.org/10.1016/j.yexcr.2013.04.023

Lapébie, P., Ruggiero, A., Barreau, C., Chevalier, S., Chang, P., Dru, P., … Momose, T. (2014). Differential responses to Wnt and PCP disruption predict expression and developmental function of conserved and novel genes in a cnidarian. *PLoS Genetics*, *10*(9), e1004590.

Leclère, L., Copley, R. R., Momose, T., & Houliston, E. (2016). Hydrozoan insights in animal development and evolution. *Current Opinion in Genetics & Development*, Vol. 39, pp. 157–167. https://doi.org/10.1016/j.gde.2016.07.006

Leclère, L., Horin, C., Chevalier, S., Lapébie, P., Dru, P., Peron, S., … Copley, R. R. (2019). The genome of the jellyfish Clytia hemisphaerica and the evolution of the cnidarian life-cycle. *Nature Ecology & Evolution*, *3*(5), 801–810.

Lecuit, T., & Yap, A. S. (2015). E-cadherin junctions as active mechanical integrators in tissue dynamics. *Nature Cell Biology*, *17*(5), 533–539.

Lee, J.-Y., Marston, D. J., Walston, T., Hardin, J., Halberstadt, A., & Goldstein, B. (2006). Wnt/Frizzled signaling controls C. elegans gastrulation by activating actomyosin contractility. *Current Biology: CB*, *16*(20), 1986–1997.

LeGoff, L., & Lecuit, T. (2015). Mechanical Forces and Growth in Animal Tissues. *Cold Spring Harbor Perspectives in Biology*, *8*(3), a019232.

Leptin, M., & Grunewald, B. (1990). Cell shape changes during gastrulation in Drosophila. *Development* , *110*(1), 73–84.

Magie, C. R., Daly, M., & Martindale, M. Q. (2007). Gastrulation in the cnidarian Nematostella vectensis occurs via invagination not ingression. *Developmental Biology*, *305*(2), 483–497.

Marcellini, S., Technau, U., Smith, J. C., & Lemaire, P. (2003). Evolution of Brachyury proteins: identification of a novel regulatory domain conserved within Bilateria. *Developmental Biology*, *260*(2), 352–361.

Marlow, H.Q., Martindale, M.Q., 2007. Embryonic development in two species of scleractinian coral embryos: *Symbiodinium* localization and mode of gastrulation. Evol. Dev. 9(4), 355–367.

Marston, D. J., Higgins, C. D., Peters, K. A., Cupp, T. D., Dickinson, D. J., Pani, A. M., … Goldstein, B. (2016). MRCK-1 Drives Apical Constriction in C. elegans by Linking Developmental Patterning to Force Generation. *Current Biology: CB*, *26*(16), 2079–2089.

Mason, F. M., Tworoger, M., & Martin, A. C. (2013). Apical domain polarization localizes actin–myosin activity to drive ratchet-like apical constriction. *Nature Cell Biology*, *15*(8), 926–936.

Matthews, A., 1917. The development of *Alcyonium digitatum* with some notes on the early colony formation. Quart. J. Microsc. Sci. 62, 43–94.

Metschnikoff, E., 1886. Embryologische Studien an Medusen. Ein Beitrag zur Genealogie der Primitiv-Organe, Wien: Alfred Holder / von Elias Metschnikoff. https://doi.org/10.5962/bhl.title.5982

Miller, C. J., & Davidson, L. A. (2013). The interplay between cell signalling and mechanics in developmental processes. *Nature Reviews. Genetics*, *14*(10), 733–744.

Moeendarbary, E., & Harris, A. R. (2014). Cell mechanics: principles, practices, and prospects. *Wiley Interdisciplinary Reviews. Systems Biology and Medicine*, *6*(5), 371–388.

Momose, T., Derelle, R., & Houliston, E. (2008). A maternally localised Wnt ligand required for axial patterning in the cnidarian Clytia hemisphaerica. *Development* , *135*(12), 2105–2113.

Momose, T., & Houliston, E. (2007). Two oppositely localised frizzled RNAs as axis determinants in a cnidarian embryo. *PLoS Biology*, *5*(4), e70.

Momose, T., Kraus, Y., & Houliston, E. (2012). A conserved function for Strabismus in establishing planar cell polarity in the ciliated ectoderm during cnidarian larval development. *Development*, *139*(23), 4374–4382.

Muller-Cale, K., 1914. Zur Entwicklunggeschichte einiger Thecaphoren, Zool. Jahrb., Abt. Anat. Ontog. Tiere 37, 83–112.

Nakaya, Y., & Sheng, G. (2008). Epithelial to mesenchymal transition during gastrulation: an embryological view. *Development, Growth & Differentiation*, *50*(9), 755–766.

Pearl, E. J., Li, J., & Green, J. B. A. (2017). Cellular systems for epithelial invagination. *Philosophical Transactions of the Royal Society of London. Series B, Biological Sciences*, *372*(1720). https://doi.org/10.1098/rstb.2015.0526

Pelham, R. J., Jr, & Wang, Y. l. (1999). High resolution detection of mechanical forces exerted by locomoting fibroblasts on the substrate. *Molecular Biology of the Cell*, *10*(4), 935–945.

Poujade, M., Grasland-Mongrain, E., Hertzog, A., Jouanneau, J., Chavrier, P., Ladoux, B., … Silberzan, P. (2007). Collective migration of an epithelial monolayer in response to a model wound. *Proceedings of the National Academy of Sciences of the United States of America*, *104*(41), 15988–15993.

Pukhlyakova, E., Aman, A. J., Elsayad, K., & Technau, U. (2018). β-Catenin–dependent mechanotransduction dates back to the common ancestor of Cnidaria and Bilateria. *Proceedings of the National Academy of Sciences of the United States of America*, *115*(24), 6231–6236.

Pukhlyakova E.A., Kirillova A.O., Kraus Y.A., Zimmermann, B., & Technau, U. (2019).A cadherin switch marks germ layer formation in the diploblastic sea anemone Nematostella vectensis. *Development* 146. doi:10.1242/dev.174623

Rauzi, M., Krzic, U., Saunders, T. E., Krajnc, M., Ziherl, P., Hufnagel, L., & Leptin, M. (2015). Embryo-scale tissue mechanics during Drosophila gastrulation movements. *Nature Communications*, *6*, 8677.

Röttinger, E., Dahlin, P., & Martindale, M. Q. (2012). A Framework for the Establishment of a Cnidarian Gene Regulatory Network for “Endomesoderm” Specification: The Inputs of ß-

Catenin/TCF Signaling. *PLoS Genetics*, Vol. 8, p. e1003164. https://doi.org/10.1371/journal.pgen.1003164

Savagner, P. (2001). Leaving the neighborhood: molecular mechanisms involved during epithelial-mesenchymal transition. *BioEssays: News and Reviews in Molecular, Cellular and Developmental Biology*, *23*(10), 912–923.

Sawyer, J. M., Harrell, J. R., Shemer, G., Sullivan-Brown, J., Roh-Johnson, M., & Goldstein, B. (2010). Apical constriction: a cell shape change that can drive morphogenesis. *Developmental Biology*, *341*(1), 5–19.

Scholz, C. B., & Technau, U. (2003). The ancestral role of Brachyury: expression of NemBra1 in the basal cnidarian *Nematostella vectensis* (Anthozoa). *Development Genes and Evolution*, *212*(12), 563–570.

Sherrard, K., Robin, F., Lemaire, P., & Munro, E. (2010). Sequential activation of apical and basolateral contractility drives ascidian endoderm invagination. *Current Biology: CB*, *20*(17), 1499–1510.

Shook, D., & Keller, R. (2003). Mechanisms, mechanics and function of epithelial-mesenchymal transitions in early development. *Mechanisms of Development*, *120*(11), 1351–1383.

Shook, D. R., Kasprowicz, E. M., Davidson, L. A., & Keller, R. (2018). Large, long range tensile forces drive convergence during Xenopus blastopore closure and body axis elongation. *eLife*, *7*. https://doi.org/10.7554/eLife.26944

Solnica-Krezel, L., & Sepich, D. S. (2012). Gastrulation: making and shaping germ layers. *Annual Review of Cell and Developmental Biology*, *28*, 687–717.

Steinmetz, P. R. H. (2019). A non-bilaterian perspective on the development and evolution of animal digestive systems. *Cell and Tissue Research*, *377*(3), 321–339.

Steinmetz, P. R. H., Aman, A., Kraus, J. E. M., & Technau, U. (2017). Gut-like ectodermal tissue in a sea anemone challenges germ layer homology. *Nature Ecology & Evolution*, *1*(10), 1535–1542.

Stower, M. J., & Bertocchini, F. (2017). The evolution of amniote gastrulation: the blastopore-primitive streak transition. *Wiley Interdisciplinary Reviews. Developmental Biology*, *6*(2), e262.

Tambe, D. T., Hardin, C. C., Angelini, T. E., Rajendran, K., Park, C. Y., Serra-Picamal, X., … Trepat, X. (2011). Collective cell guidance by cooperative intercellular forces. *Nature Materials*, *10*(6), 469–475.

Tamulonis, C., Postma, M., Marlow, H. Q., Magie, C. R., de Jong, J., & Kaandorp, J. (2011). A cell-based model of Nematostella vectensis gastrulation including bottle cell formation,

invagination and zippering. *Developmental Biology*, *351*(1), 217–228.

Technau, U. (2001). Brachyury, the blastopore and the evolution of the mesoderm. *BioEssays*, Vol. 23, pp. 788–794. https://doi.org/10.1002/bies.1114

Thomas, M. B., Freeman, G., & Martin, V. J. (1987). The Embryonic Origin of Neurosensory Cells and the Role of Nerve Cells in Metamorphosis in Phialidium gregarium (Cnidaria, Hydrozoa). *International Journal of Invertebrate Reproduction and Development*, *11*(3), 265–285.

Wallingford, J. B., Fraser, S. E., & Harland, R. M. (2002). Convergent extension: the molecular control of polarized cell movement during embryonic development. *Developmental Cell*, *2*(6), 695–706.

Williams, M. L., & Solnica-Krezel, L. (2017). Regulation of gastrulation movements by emergent cell and tissue interactions. *Current Opinion in Cell Biology*, *48*, 33–39.

Figure 1. Cleavage divisions to form the early blastula

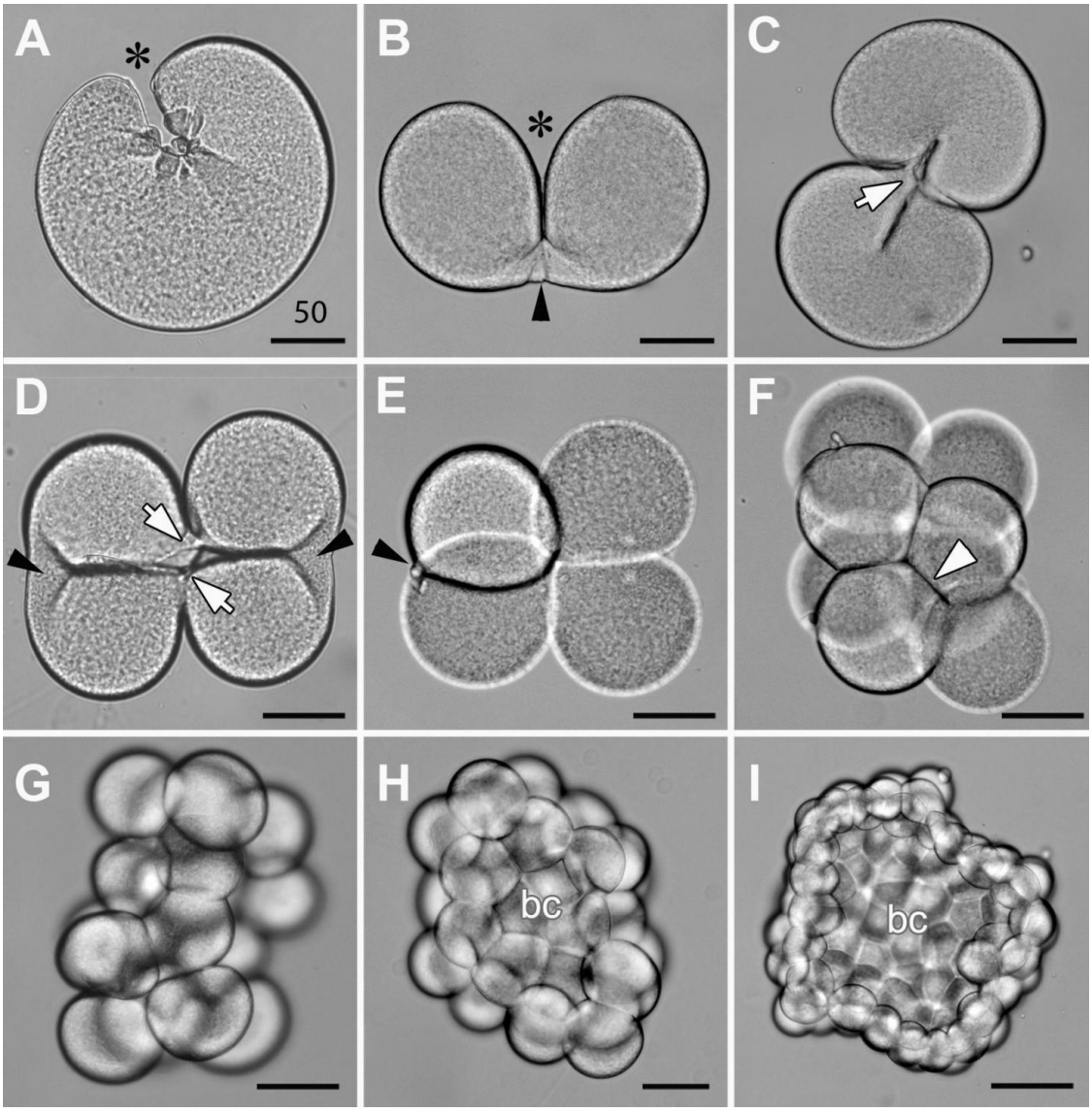

Light microscopy images of living embryos. (A) Initiation of the first cleavage furrow: asterisk marks the site of furrow initiation, corresponding to the egg animal pole. (B) Elongation of the first cleavage furrow. Black arrowhead points to the cytoplasmic bridge between the forming blastomeres. (C, D, E) Transition between two-cell stage and four-cell stage, viewed from the animal pole. Two second cleavage furrows start to form in (C). White arrows mark lamellae connecting the non-sister blastomeres. Forming blastomeres often "twist" against each other as the furrow advances, resulting in tetrahedron arrangements as in (E). (F) Eight-cell stage embryo with blastomeres in this example showing a pattern reminiscent of spiral cleavage. The cell arrangement is variable between embryos. Arrowheads points to contacts between non-sister blastomeres. (G) 16-cell stage. (H) 32-cell stage, appearance of the blastocoel (bc). (I) 128-cell stage. All scale bars - 50 um.

Figure 2. Development from the late blastula to the planula stage

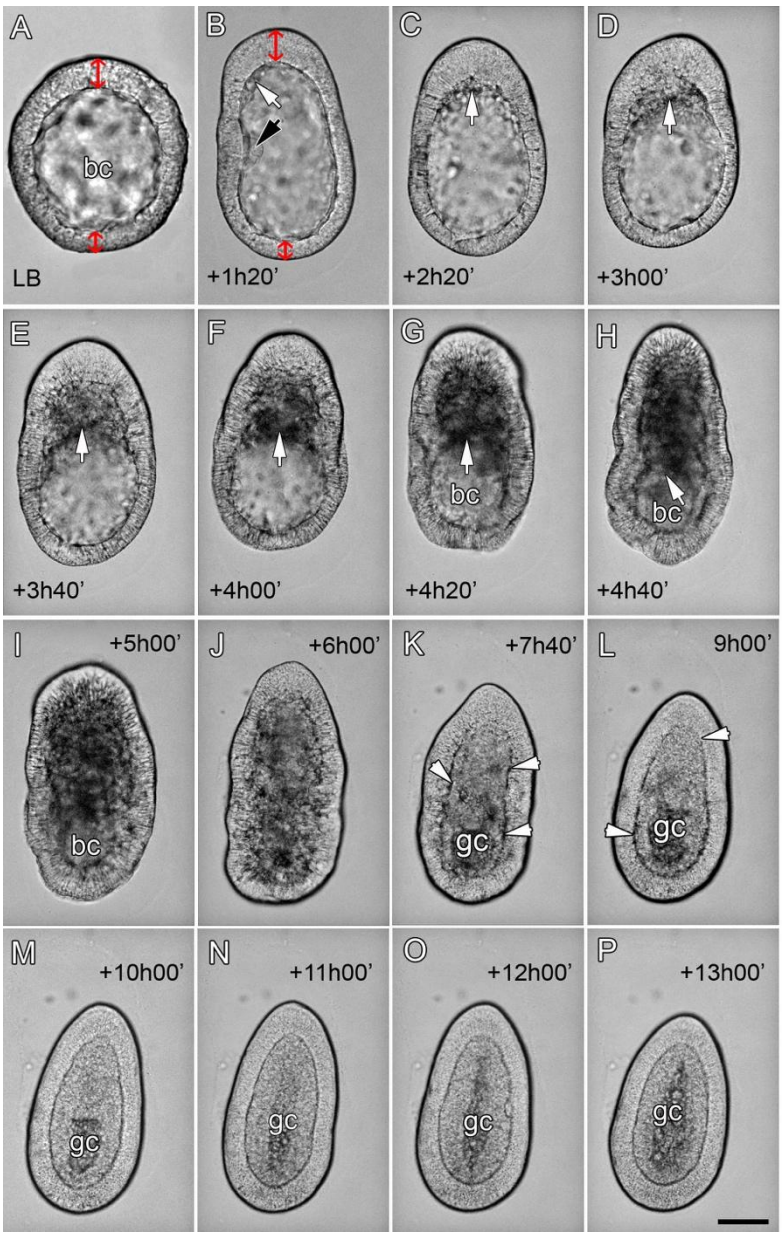

Light microscopy images of live embryos; oral pole at the top in all cases. (A) Embryo at the late blastula stage; thickening of the oral half blastoderm relative to the oral blastoderm, indicated by double-headed arrows, is the first morphological sign of the OA axis. (B - P) Frames taken from a time-lapse movie of an individual gastrulating embryo encapsulated in low melting point agarose. The time from the time of embedding at the early gastrula stage on the microscope stage at around 20°C is indicated in each frame. This embryo shows atypically exaggerated elongation along the OA axis, due to the inclusion procedure. (B) Early gastrula stage, at the very beginning of gastrulation. White arrow points to the first ingressing cells. Black arrow points to a blastoderm fold which arose during cleavage. (C - I) Successive stages of gastrulation. White arrows point to the front of the mass of ingressed cells moving towards the aboral pole. Note a gradual reduction of the blastocoel (bc). (J) Parenchymula stage. Gastrulation is complete; blastocoel is filled with ingressed cells. (K - P). Development of the planula larva. White arrowheads point to the forming basal lamina separating the germ layers. A gastrocoel (gc) starts to form in the aboral endoderm and spreads towards the oral pole as ingressed cells reorganize to form a gastrodermal epithelium. Note the distinct oral/posterior (pointed) and aboral/anterior (rounded) poles of the larva. Scale bar 50 µm

Figure 3. Gross morphology and cell morphology of blastula stage embryos

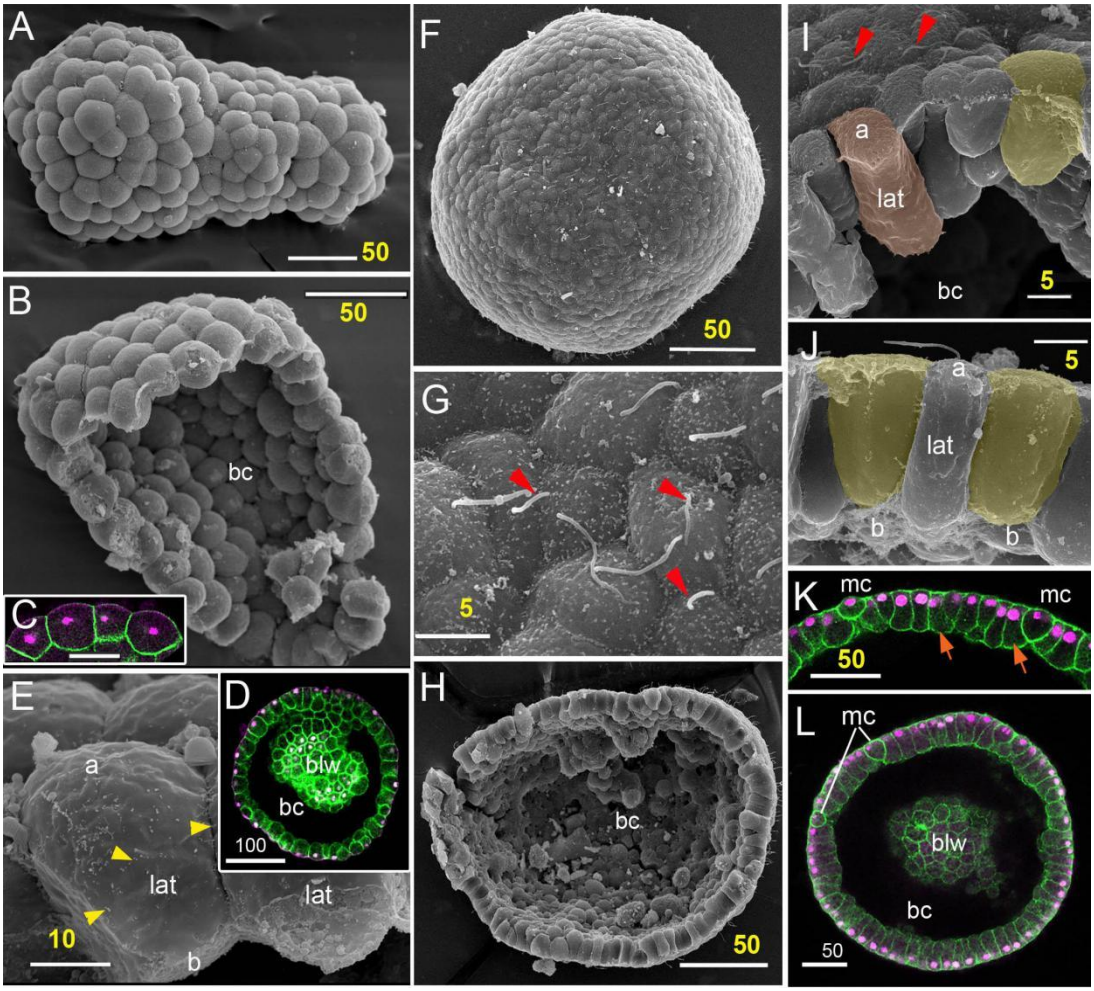

(A) SEM of an embryo at the early blastula stage (256 - 512 cells), with an irregular, non-spherical shape. (B) SEM of an early blastula split into two. Blastoderm cells have a rounded shape. (C) CLSM z-plane of early blastula cells. In this and in all other CLSM images, actin-rich cell cortices are labeled with phalloidin (green) and nuclei with Hoechst dye (magenta). Cell shapes are irregular and nuclei central; bc - blastocoel. (D, E) CLSM (D) of an embryo at the mid-blastula stage and SEM (E) of cells from a split embryo fixed at the same stage. The embryo shape has become more regular. Cells have elongated slightly along the apico-basal axis and nuclei are displaced to the apical pole of each cell; short filopodia (yellow arrowheads) cover the lateral cell surface providing the cell-cell contacts; a - apical, lat - lateral, b - basal cell surfaces, blw - blastocoel wall. (F-L) Late blastula stage. SEM (F-J) and CLSM (K, L) showing further epithelialization. F) Surface view of an embryo, whose shape is close to spherical. (G) Same embryo at higher magnification. Each cell has a cilium (red arrowhead). (H) An embryo split into two. Cells are columnar and organized in an epithelium. (I, J, K) Blastoderm cells showing a variety of shapes. A cell with an expanded basal domain in I is highlighted in orange; a cell with a tapered basal end (left) and one with a cylindrical form (right) are highlighted in yellow in (J). Orange arrows in (K) indicate cells with expanded basal domains; mc - rounded mitotic cells. (L) CLSM image illustrating further elongation of blastoderm cells along the apico-basal axis compared to the mid-blastula stage. Scale bars: A, B, F, H, K, L - 50µm; C - 25µm; D - 100µm; E - 10µm; G, I, J - 5µm.

Figure 4. Scheme of cell shape changes during *Clytia* early development.

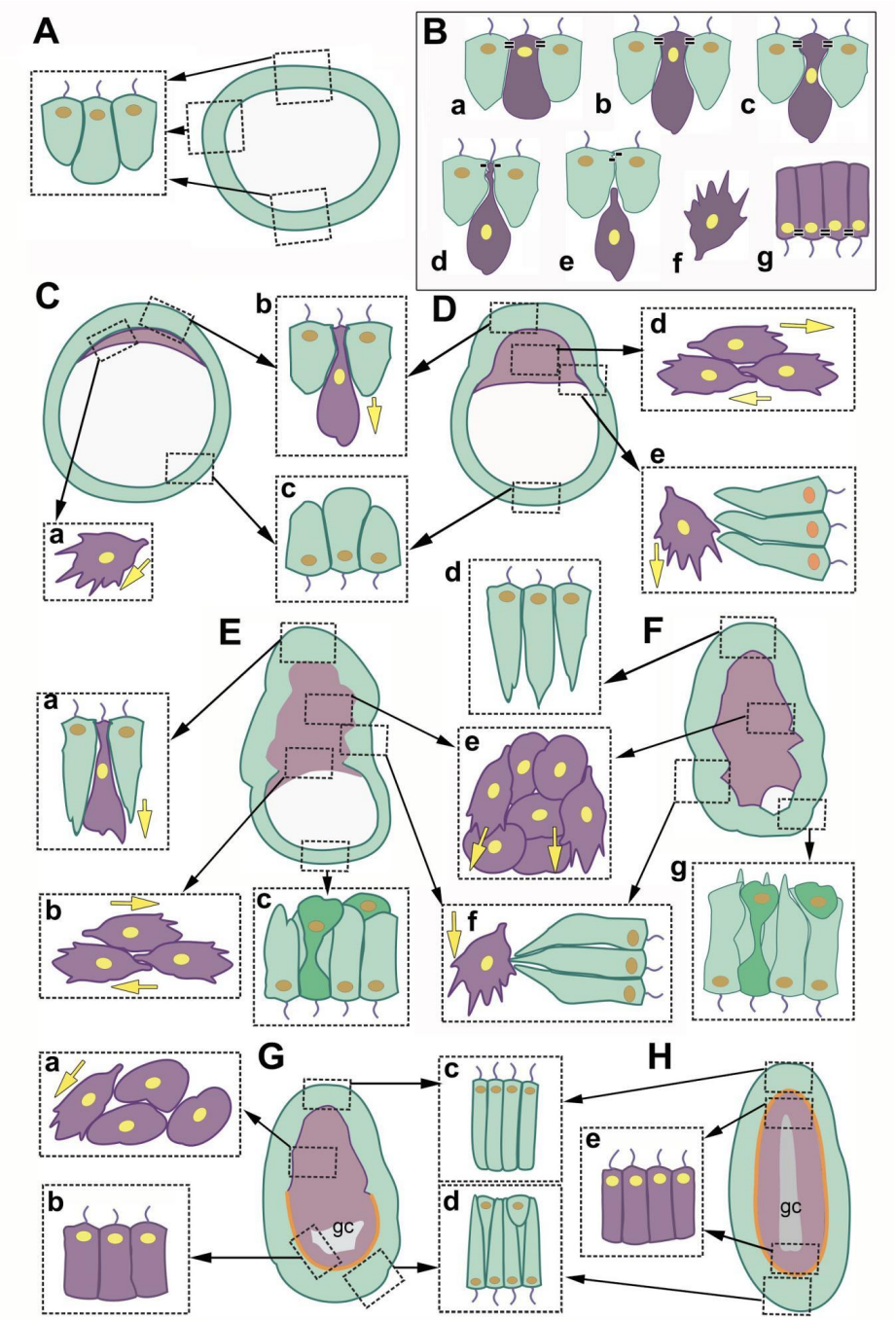

The cartoons in A and C-H show overviews of the cell shapes in different regions of embryos at successive stages of gastrulation, while B follows the changes in individual endoderm fate cells across these stages. Embryos stages: (A) late blastula, (C) Early gastrula, (D) mid-gastrula, (E) late gastrula, (F) late gastrula, during completion of blastocoel reduction, (G) parenchymula with gastrocoel formation starting, (H) 2 day planula. (B) Successive stages of bottle cell formation (a - d), ingression (e, f) and incorporation into the epithelial endoderm (g). The outer cell layer containing the presumptive ectoderm and presumptive endoderm cells (A-E) or exclusively ectoderm cells (F - H) is in green; presumptive endoderm is in violet; basal lamina (G, H) is in orange; yellow arrows show directions of movements of the future endodermal cells; gastrocoel (G, H) is in light gray

.

Figure 5. Early gastrula stage: distinct cell morphologies in the oral domain

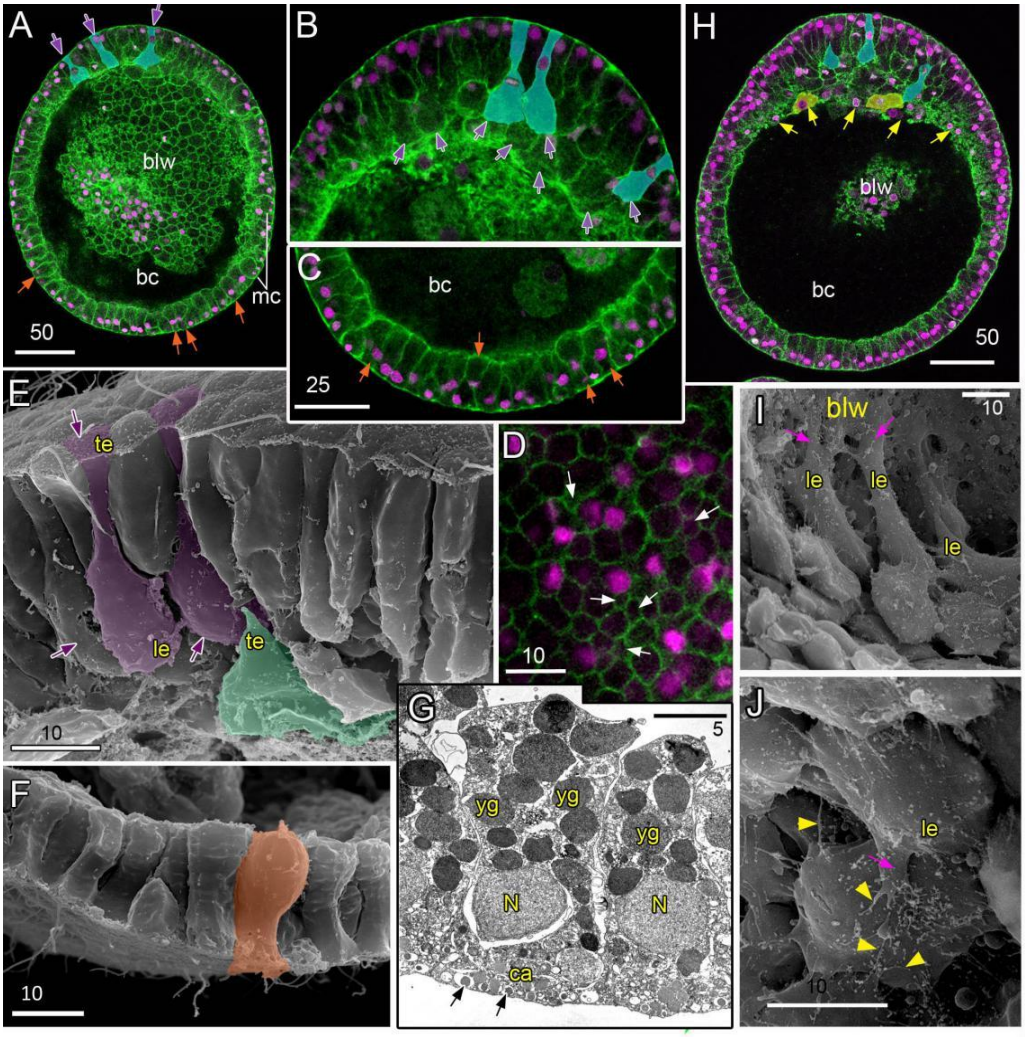

(A - D) CLSM images of embryos at the very beginning of gastrulation, before any cells have entered the blastocoel. The oral pole is towards the top in all images. In the oral blastoderm (A, B), violet arrows indicate bottle cells characterized by elongated apico-basal axes, contracted apical surfaces and expanded basal surfaces. Cells highlighted in turquoise illustrate bottle cells at different stages leading to ingression, as indicated by the location of the nuclei in apical or central positions. These stages are characterized further in Figure 5. In the aboral blastoderm (A, C), orange arrows indicate cells with expanded basal areas, morphologically resembling bottle cells. (D) Confocal plane parallel and close to the apical surfaces of aboral cells, showing a wide range of apical surface areas. (E, F) SEM of oral (E) and aboral (F) cells of split embryos at an equivalent very early gastrula stage. Oral bottle cells are highlighted in violet and a cell already ingressed into the blastocoel in green. An aboral cell with an expanded basal area is highlighted in orange; le - leading, te - trailing edges of bottle cells preparing to ingress. (G) TEM of aboral cells in an equivalent embryo stage; N - nucleus, yg - yolk granules, ca - cortical area, black arrows point to the cortical granules. (H) CLSM of an early gastrula embryo demonstrating ingression of oral cells has now commenced. Some ingressed cells (yellow arrows) have started to migrate inside the blastocoel. (I) Ingressed cells migrating over the blastocoel wall. Their leading edges (le) are very pronounced and form wide lamellae (magenta arrows). (J) Ingressed cells located further from the blastocoel wall have small lamella and multiple filopodiae (yellow arrowheads). Scale bars: A, H - 50 µm; B, C - 25 µm; D, E, F, I, J - 10 µm; G - 5 µm.

Figure 6. Morphology and ultrastructure of bottle cells at the early gastrula stage

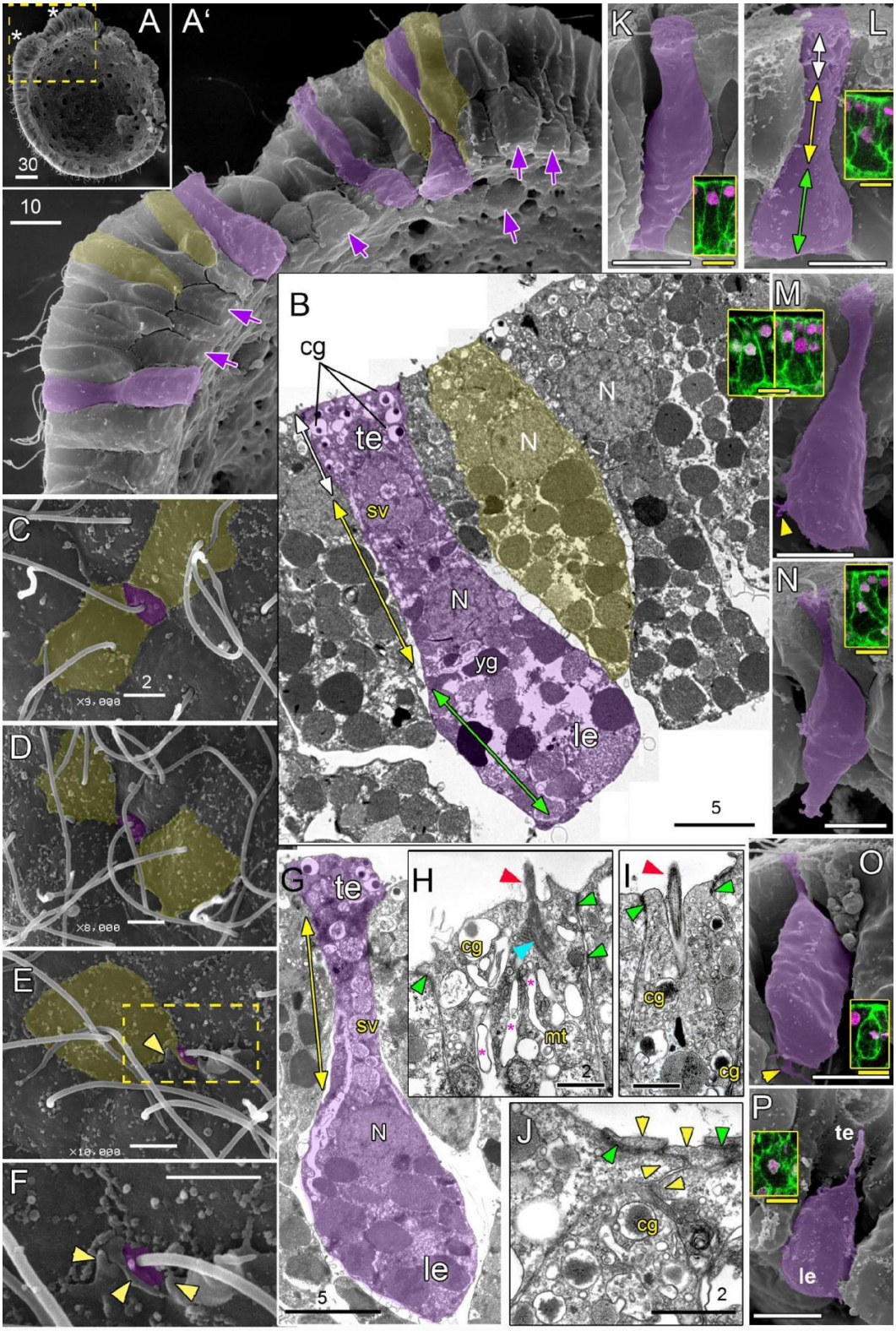

(A) SEM image showing the cut surface of an embryo fixed and split at the early gastrula stage; two areas of cell ingression are marked with the asterisks. (A') Zoom on the oral area framed in (A). Multiple bottle cells (violet color, violet arrows) alternate with columnar cells with relatively short apico-basal axes ("squat cells" yellow color). (B) TEM of the early gastrula oral area: two forming bottle cells (one colored in violet) and two squat cells with

short apico-basal axes (one colored in yellow). The bottle cell nucleus is positioned distant from the contracted apical domain (white double-headed arrow), near the expanded basal domain (green double-headed arrow) in the 'neck' region between the apical and basal areas (yellow double-headed arrow). Cortical granules (cg) are displaced deeper into the apical cytoplasm. N= nuclei; te= trailing edge; sv= putative storage vesicles; yg= yolk granules; le= leading edge. (C - F) SEM of the oral surface of an embryo. (F) zoom on the area framed in (E). Successive stages of the 'sinking' of ingressing bottle cells; apical surfaces of bottle cells are highlighted in violet and of neighboring epithelial cells in yellow. Yellow arrowheads point to filopodia-like protrusions of epithelial cells extending over the surface of the sinking bottle cells. (G) TEM of a bottle cell at a later stage of ingression than the cell shown in (B): the 'neck' (yellow double-headed arrow) is now narrower than the cell apex and the nucleus (N) is displaced into the expanded basal area; storage vesicles (sv) are lined up along the cell neck. (H - J) TEMs of the apical domains of bottle cells at three stages of cell ingression. (H) At the beginning of ingression, bottle cell retains the cilium (red arrowhead, with blue arrowhead pointing to the cilium root) and sub-apical intercellular junctions (green arrowheads). Note the elongated shape of vacuoles (marked with stars) squeezed by the apical contraction; mt= mitochondria. (I) The next stage of apical contraction: the cilium is deeper within a 'pocket' formed from the apical cell membrane; intercellular junctions are still preserved. (J) Apical domain of a cell that has already ingressed, covered by protrusions of neighboring epithelial cells closing the 'hole' at the place of ingression (yellow arrowheads). Well-developed intercellular junctions (green arrowheads) are present between these protrusions. (K - P) Successive stages of bottle cell reshaping during ingression, SEM and CLSM images. At the beginning, the cell apex is already slightly contracted and the nucleus is located apically (K). At the next step, the 'neck' becomes longer and narrower than the apical surface; the nucleus is displaced into the neck (K - M). When the apex contracts further the cell neck becomes narrower and slightly contracts too (N). The neck contracts further and the nucleus is positioned in the basal part of the cell (O). The cell loses the contacts with neighboring cells and ingresses into the blastocoel (P). Note the protrusions (yellow arrowheads) on the basal surfaces of bottle cells. Scale bars: A - 30μm, A' - 10μm; B and G - 5μm; C - F and H - J - 2μm; K - P - 10μm (white scale bars - SEM images; yellow scale bars - CLSM images).

Figure 7. The mid-gastrula stage: continued cell ingression, migration of ingressed cells

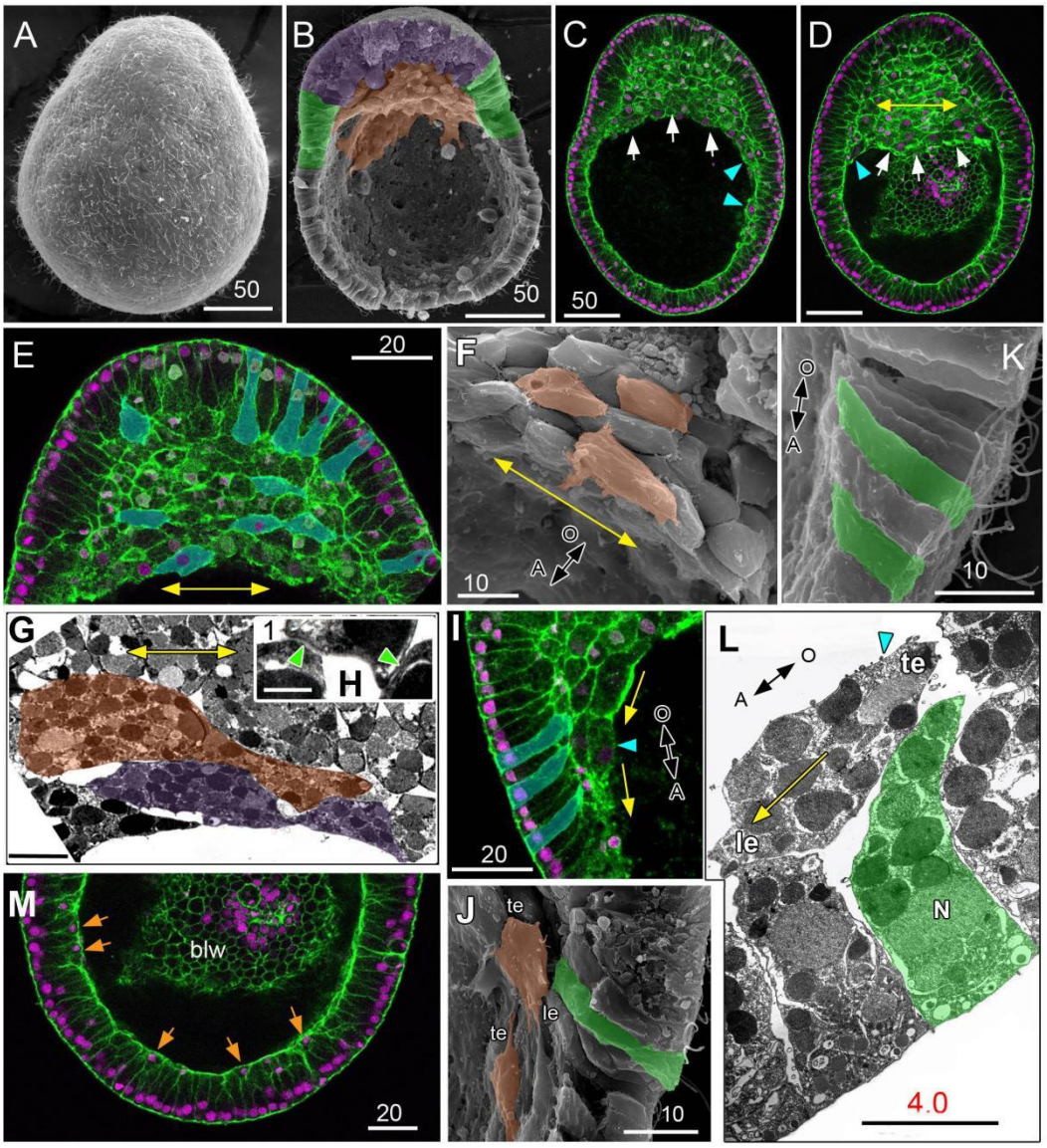

Mid-gastrula stage embryos positioned with their pointed oral poles towards the top in all panels. (A) SEM image, side view. (B, C ,D) Successive stages of cell ingression illustrated on the exposed face of a split embryo(B) and CLSM medial z-planes (C,D) . The zone of cell ingression in (B) is colored in purple; the mass of ingressed cells in orange. The 'belt' area of the blastocoel wall, colored in green, aligns with the front of the ingressed cells mass. In (C,D) this front is labelled with white arrows; cyan arrows point at individual cells migrating over the blastocoel wall; yellow double-headed arrow indicates the preponderant direction of cell movements within the ingressing mass. These cells intercalate between each other, aligning as layers with their individual long axes perpendicular to the embryo oral –aboral axis. (E) CLSM of the oral area of an embryo at the mid-gastrula stage. Bottle cells and individual cells of the cell mass are highlighted in blue. (F - H): SEM (F) and TEM (G, H) of the aboral-most portion of the mass of ingressed cells. Individual ingressed cells are highlighted in orange and purple (F, G). Green arrowheads show spot-like sites of adhesion between the migrating cells (H). (I, J, K, L): CLSM (I), SEM (J, K) and TEM (L) of the 'belt' area. The marginal cells of the cell mass (cyan arrowheads) move over the basal surfaces of the blastocoel wall cells (yellow arrows show the direction of this movement). The blastocoel wall cells in the belt area are highlighted in blue in (I) and in green in (J, K, L); these cells are bent, and their basal ends

slant up towards the oral pole. (M) - CLSM of the blastocoel roof; orange arrows point to cells with basally located nuclei. Scale bars: A - D - 50μm; E, I, M - 20μm; G - 5μm; H - 1 μm; F, J, K - 10μm; L - 4μm.

Figure 8. The late gastrula stage and transition to parenchymula stage.

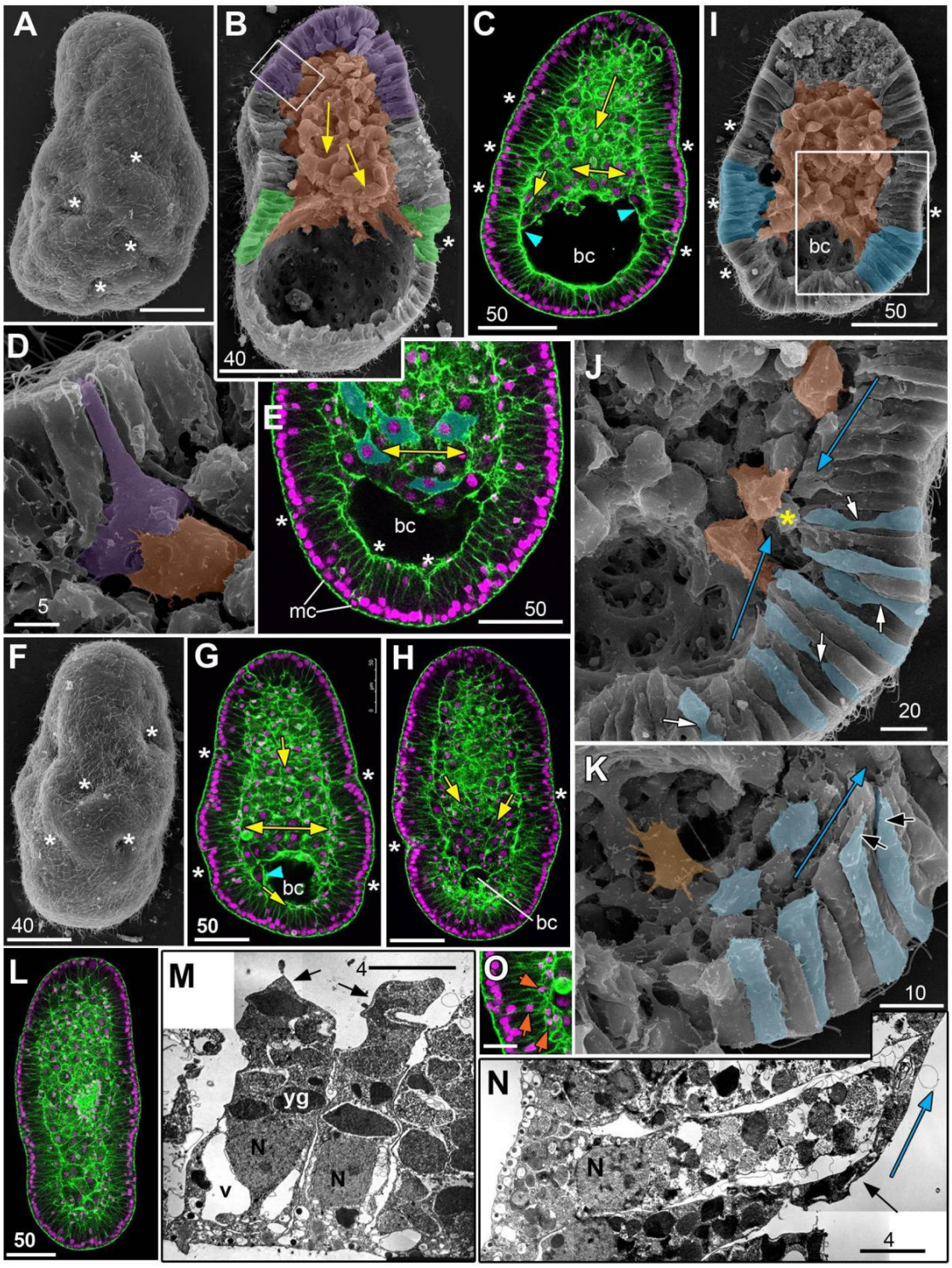

(A) - An embryo at the late gastrula stage (SEM image, side view). Note multiple wrinkles and folds (white asterisks) at the embryo surface, especially the aboral half. (B) - SEM image of a split late gastrula stage embryo. Yellow arrows show the direction of cell movements in the mass of ingressed cells, highlighted in brown. A fold-rich region of presumptive ectoderm

cells overlying the front of migrating inner cells, the belt area, is highlighted in green and the oral pole region of cell ingression in purple. (C) - high magnification of the area framed in (B). Cell ingression is still in progress. A bottle cell is highlighted in purple; and an individual ingressed cell in orange. (B, D, E, F, G, L) - Successive stages of blastocoel reduction imaged by CLSM. Note that only aboral front cells of the cell mass align as layers (double-headed arrows on D, E), and other cells form streams oriented towards the aboral pole (yellow arrows in B, D, E, G). Marginal cells of the cell mass move over the blastocoel wall outpacing the front of the cell mass (cyan arrowheads in B, D, F). Cell alignment in the endodermal mass at the final steps of blastocoel reduction is less pronounced, as the cell mass becomes narrower perpendicular to the oral-aboral axis and relatively higher number of cells become peripheral cells, which align with the blastocoel (G). (H) - SEM image of an embryo at the end of the blastocoel reduction. The shape difference between the oral and aboral halves is less pronounced than in (A). (I, J, K) - morphology of the presumptive ectoderm cells at the late gastrula stage, SEM images. (I) Cells of two folds aligned with the front of underlying migrating cells are highlighted in blue. (J) High magnification of the area framed in (I); cells of different shapes (side view) are highlighted in blue. Blue arrows show the tilt of the apico-basal axes in cells of a fold. The inner tip of the fold is marked with a yellow asterisk. White arrows point to the cells with expanded basal parts and narrow necks connecting the basal and apical parts. (K) SEM image demonstrating the cell basal surfaces. Black arrows point to elongated basal ends slanted to the tip of a fold. Individual cells lining the blastocoel highlighted in brown arise from the migrating cell mass. (L) SEM of an embryo at the parenchymula stage with the blastocoel completely filled with ingressed cells. (M) TEM of the aboral cells of the same stage embryo as shown in (B); black arrows point to the cell basal ends. (N) TEM of the aboral cells of the same stage as shown in (I). Note the difference between the cell apico-basal lengths and cell shapes in (M) and (N). (O) CLSM of a fragment of the presumptive lateral ectoderm. Orange arrows point to the nuclei displaced to the basal area. Scale bars: A, B, F - 40μm; C, E, G, H, I, L - 50μm; D - 5μm; J, O - 20; K - 10μm; M, N - 4μm.

Figure 9. Formation of the planula. Epithelization of the endoderm and cell differentiation

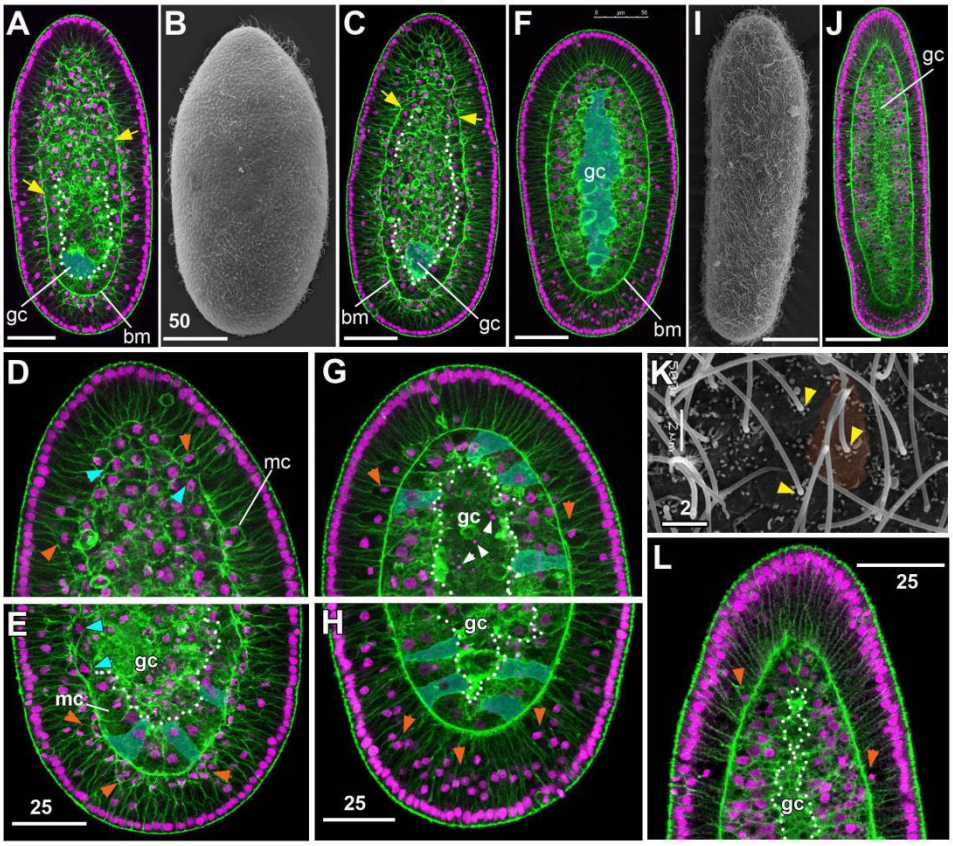

Developing planulae 1 (A-E), 2 (F-H) and 3 (I-L) days after fertilization with oral poles at the top in all panels. (A, B) CLSM and SEM of embryos at the beginning of the gastrocoel formation. A small gastrocoel (gc) appears first near the aboral pole (highlighted). The basal lamina (bl) and an epithelial endoderm start to form in the aboral half. Yellow arrows indicate the oral limit of the basal lamina visible on the CLSM section in (A); white dots outline the forming enodermal epithelium. (C) In this embryo the basal lamina has extended further towards the oral pole. (D, E) High magnification of the oral (D) and aboral (E) areas of the embryo shown in (C). Cyan arrowheads point to endodermal cells with a spindle shape in cross-section characteristic of migrating cells. Orange arrowheads point to the ectodermal cells with the basally located nuclei. Note the basally and apically localized mitotic cells (mc) in (D) and an endodermal mitotic cell in (E). Individual epithelial cells in the endoderm are highlighted in blue in (E). (F) Early planula (2 days post fertilization). Gastrocoel formation and endoderm epithelization are complete. (G, H) High magnification of the oral (G) and aboral (H) areas of the embryo shown in (F). Individual epithelial cells in the endoderm are highlighted. White arrowheads point to the small DNA-containing bodies, presumably fragmented nuclei of dead cells. The number of ectodermal cells with basally and centrally positioned nuclei is much higher in the aboral area (compare G and H), reflecting the differentiation of multiple cell types in the aboral pole ectoderm at this stage. (I, J) Mature planulae (3 days following fertilization) with an elongated body, pointed oral (posterior) pole and rounded aboral (anterior) pole. (K) Apical surfaces of the planula ectoderm cells. One of these cells is highlighted in orange. Yellow arrowheads point to the cilia. All the cilia are positioned towards the aboral (anterior) side of the cells. (L) High magnification of the planula oral (= posterior) pole. Scale bars: A, B, C, F, I, J - 50μm; D, E, G, H, L - 25μm; K - 2μm.

Figure 10. Expression of regulatory and territory marker genes during gastrulation

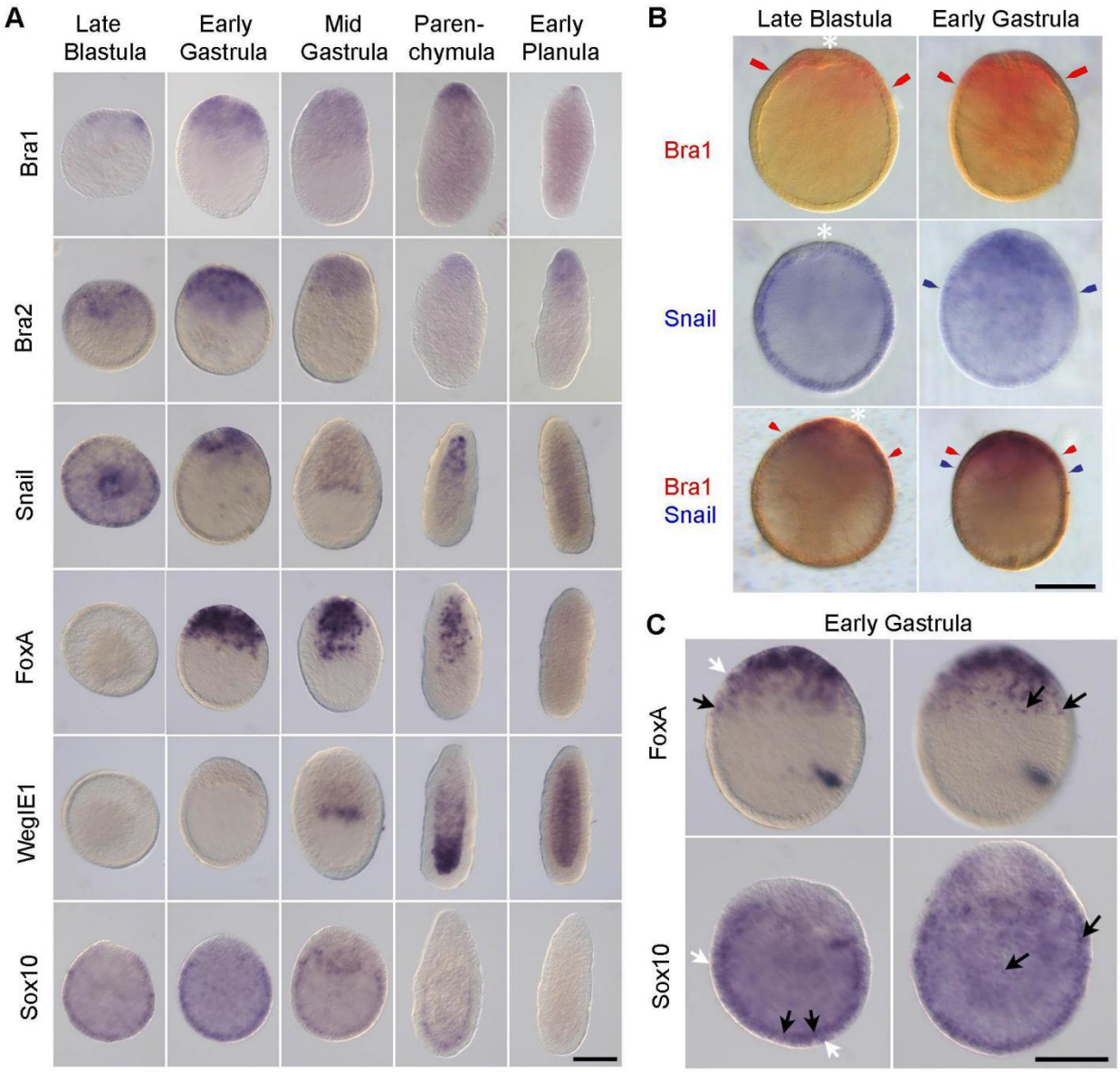

(A) In situ hybridization detection of CheBra1, CheBra2, CheSnail, CheFoxA, CheWegIE2, and CheSox10 mRNAs at the late blastula, early gastrula, mid-gastrula, parenchymula (1 day pf) and planula (2 day pf) stages. as indicated by labels on the left and top of the panel. (B) Double in situ hybridization detection of *CheBra1*(red), and *CheSnail* (blue) expression at late blastula and early blastula stages. Red and blue arrows indicate the aboral limit of Bra1 and Snail expression, respectively. At the blastula stage Snail expression is mainly uniform, but 'holes' of low expression for each gene coincide at the oral pole (white asterisks). (C) Detection of FoxA (upper row) and Sox10 (bottom row) on early gastrula stage embryos. Optical sections are through the embryo center on the left, and at the level of the blastoderm basal layer on the right. Black arrows show the bulbous basal domains of oral FoxA positive bottle cells and lateral/aboral Sox10 positive cells at this level. At the embryo surface (white arrows), the thinner apical pole of FoxA positive cells can be detected, while Sox10 staining is relatively weak. Oral pole is up in all panels. Scale bars 100µm.

Figure 11. Interpretation of embryo and cell morphology during *Clytia* gastrulation in terms of forces and tensions

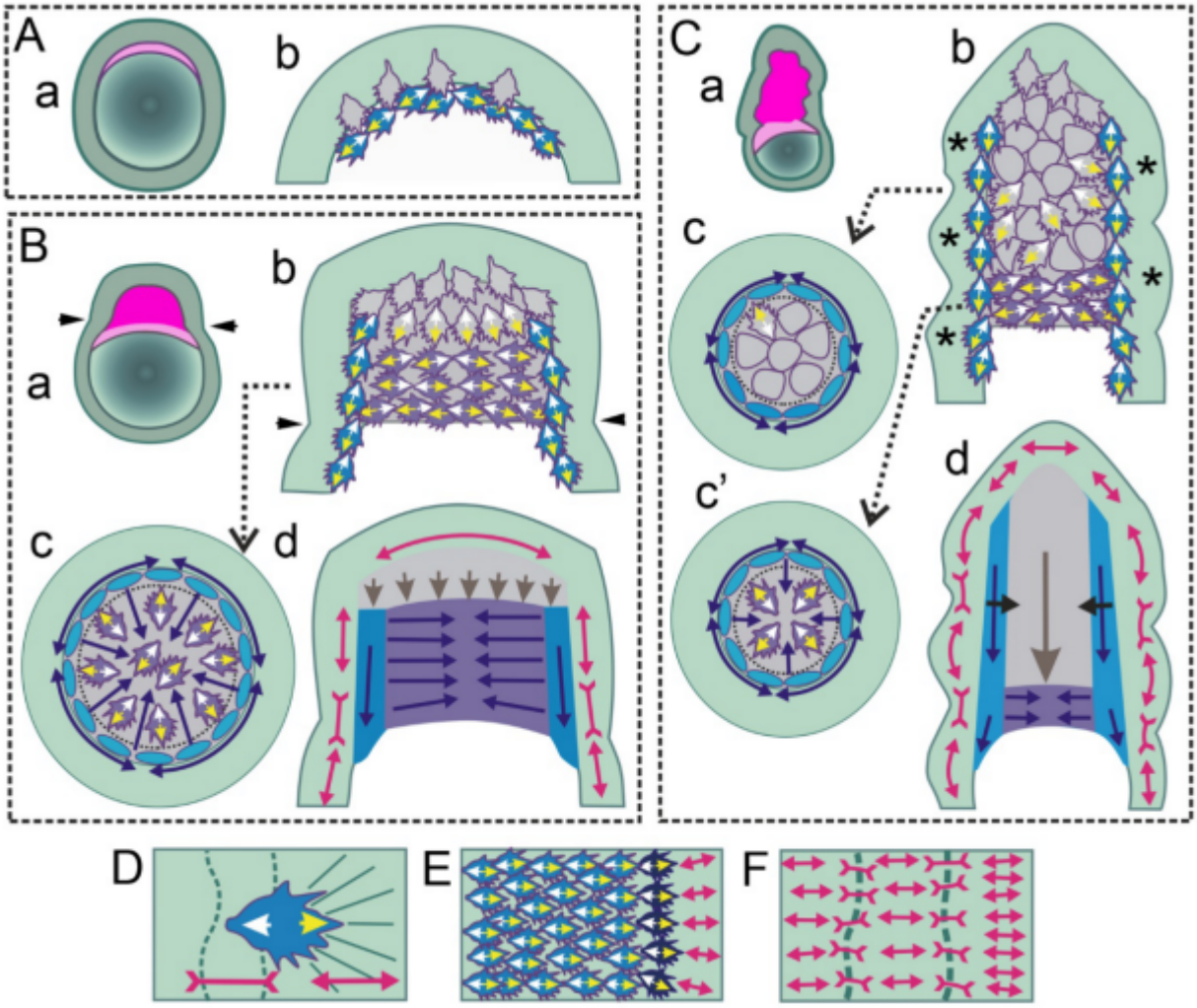

The composite panels (A :early gastrula) , (B: mid-gastrula) and (C: late gastrula) illustrate the spatial distribution of cell morphologies and movements: individual cartoons show embryo midsections with oral at the top (a), zooms on the oral end (b), cross sections at the levels indicated (c and c'), and predicted forces and tensions driving morphogenesis(d). Color codes as follows: blastoderm cells (ie ectoderm and non-ingressed presumptive endoderm) in green; Domain of ingressed presumptive endoderm are in magenta, with the earliest-ingressed in a lighter shade; Individual ingressing and ingressed presumptive endoderm cells in violet or in blue (=crawling cells). Dashed lines in c and c' cartoons indicate the frontier between the "shell" of crawling cells and the inner core; Yellow arrows show the direction of individual cell movement; White arrows show the traction forces exerted by the migrating cells; Grey arrows show predicted pushing forces generating by the ingressed cells; Red double-headed arrows indicate the stretching (outward pointing) and compression (inward pointing) of the blastoderm. Dark blue arrows show the tensile stresses. Black arrows in Cd show the squeezing forces exerted by the blastoderm when the diameter of oral region decreases. Arrowheads in B indicate the 'belt' area of the blastoderm. Macroscopic folds of the blastoderm in C are marked with the asterisks.

Panels D-F illustrate examples of the relationship between individual cell morphology and force predictions. (D) An individual ingressed cell of the 'shell' migrating over the blastoderm basal surface generates traction forces oriented opposite to cell migration and acting on the substrate. The blastoderm beneath the cell on its trailing side is compressed into micro-folds (dashed lines) perpendicular to the direction of motion, and ahead of migration is stretched into the radial wrinkles (solid lines). (E) Multiple cells migrating over the blastocoel wall at the mid/late gastrula stage similarly induce stretching of the area above the front of migration. Cells of the aboral front of migration are colored in dark blue. F) Blastocoel wall surface; migrating cells were removed to show alternating areas of stretching and compression. Macroscopic folds (dashed lines) correspond to the areas of compression.